vehicles

MDPI

Article

Integrated Freight Train Rescheduling and Dynamic Railcar Flow Rerouting Under Unexpected Events

Bowen Ma

Transportation & Economics Research Institute, China Academy of Railway Sciences Corporation Limited, Beijing 100081, China; mabowen@rails.cn

Abstract

Railroad daily operations can be significantly disrupted by unforeseen events such as adverse weather conditions and train accidents. These events often result in delays in delivering shipments on time. Therefore, studying how to reschedule freight trains during emergencies is essential for enhancing the competitiveness of rail transportation products. This paper proposed a method specifically designed for the rescheduling of freight trains, aiming to simultaneously modify the train operation plan and dynamically adjust railcar flow routes in response to unexpected events. The problem was formulated with a multi-objective model based on a two-layer space–time network. To accurately measure schedule deviations, we introduced a set of indicators specifically tailored to the characteristics of railroad freight transportation. The ε-constraint method was employed to establish a framework for searching three-dimensional Pareto solutions. Computational experiments were performed on a Chinese railroad network. The results validated the effectiveness and applicability of the proposed methodology.

Keywords: freight train rescheduling; train operation plan; dynamic railcar flow rerouting; space–time network; Pareto solution; ε-constraint method

1. Introduction

Rail freight transportation involves a sophisticated operational process and consumes substantial resources, including locomotives and railcars [1]. To ensure the efficient allocation of resources, which fulfills economic objectives and expedites customer service, railroads must develop comprehensive plans that cover both external and internal aspects. Externally, the railroad company presents a service plan (presented as a timetable) to potential customers. Meanwhile, internal operations, not visible to customers, involve decisions such as car routing (determining the physical route for each origin–destination shipment) [2], car-to-block assignment (deciding which blocks should be built and the serving block sequence for each OD's shipments) [3] and block-to-train assignment [4].

While the decisions above provide a strategic and tactical foundation for daily railway operations, at the operational level, railroad dispatchers must still formulate daily operation plans to regulate real-time train and railcar transportation organization. Constrained by freight capacity, many railways, including China's rail system, adopt a controlled transportation organization mode in which freight trains can depart only when minimum marshaling size requirements are satisfied. Nevertheless, conventional freight train timetables are generally compiled based on medium- and long-term freight volume forecasts [5], which cannot fully match the real-time dynamic accumulation of railcars. When the actually accumulated railcars fail to reach the target train size, pre-planned timetable schemes

Check for updates

Academic Editors: Yao Chen, Yongxiang Zhang and Jungang Shi

Received: 20 July 2026
Revised: 25 August 2026
Accepted: 1 September 2026
Published: 3 September 2026

Copyright: © 2026 by the author. Licensee MDPI, Basel, Switzerland. This article is an open access article distributed under the terms and conditions of the Creative Commons Attribution (CC BY) license.

cannot be implemented as scheduled. Accordingly, dispatchers need to develop a technical document known as the train operation plan based on dynamic railcar data before each day's work. The train operation plan comprises two main components: (1) establishing the time–space routes for freight trains, which involves determining the time schedules for trains [6], and (2) establishing the time–space routes for railcars, which involves creating transportation schemes to assign railcars to specific trains [7].

Under normal circumstances, dispatchers operate trains according to the established train operation plan. However, external and internal factors such as adverse weather conditions and malfunctions in the railroad infrastructure can lead to situations where trains are either early, late, canceled, or added [8]. As a result, railcars may fail to reach their destinations according to the established plan and could become stranded along the route. In such instances, dispatchers must promptly adjust the train operation plan to restore regular shipment transportation. However, relying solely on dispatchers' experience and subjective judgment to make temporary adjustments to the train operation plan is arbitrary. Furthermore, the railroad company has already committed to delivering the shipments within a specified deadline after accepting the order. Failing to adjust the train operation plan promptly could disrupt the on-time delivery of the shipments, which is not conducive to enhancing the competitiveness of railroads in the freight market. Therefore, there is an urgent need to propose an automated method of plan adjustment to effectively cope with the negative impact of unexpected conditions on rail freight operations.

Addressing this need is complicated by the fact that the operational environment of freight railroads varies significantly across regions, which directly shapes the rescheduling problem. In Europe, for instance, railroads typically operate on a scheduled-service basis, where trains run according to fixed timetables without strict composition requirements. In the United States, freight trains predominantly operate on dedicated freight lines. This study is situated in a mixed-traffic railway system in which freight trains are subject to minimum marshaling size requirements and their operations are tightly coupled with passenger train schedules and railcar flow movements. In this setting, because train departures depend on sufficient car accumulation while car routing must conform to available train schedules, the two decisions—adjusting train schedules and reassigning railcars to trains—are tightly interdependent and cannot be handled in isolation.

Despite this strong interdependence, the joint adjustment of these two decisions remains insufficiently addressed in the literature. Existing studies on train rescheduling have largely focused on passenger railways or treated them as separable sub-problems, overlooking their coupling in freight operations. This is partly because railcar routing at the operational level involves a richer set of activities than train scheduling alone, including the transition between loaded and empty car states, empty car distribution, and loaded car transportation, which have not been considered in prior studies. Prior service network design research [9] employed a multi-layer space–time network to characterize the movements of railcars and trains, but that work operates at the tactical level and its car layer is too simple to fully capture the car organization process, including the handling of empty cars, which renders it inadequate for daily freight operations. To bridge this gap, this paper investigates the integrated adjustment of train operation plans under disruptions. Specifically, we address the following research questions: (i) How can the coupling between freight train rescheduling and railcar-to-train reassignment be systematically modeled within an effective joint optimization framework? (ii) How can an effective trade-off between customer interests and operator interests be achieved during the adjustment process? To answer these questions, we construct a two-layer space–time network tailored to freight operations and propose a comprehensive optimization method. By refining the space–time arc types to explicitly capture the complete turnover process of railcars, this

network structure enables the simultaneous optimization of train rescheduling and railcar routing under disruptions. In particular, a three-dimensional Pareto search framework is developed to capture the trade-offs among the conflicting objectives.

The remainder of this paper is organized as follows. Section 2 reviews the related literature. Section 3 presents the problem description, model formulation, and solution algorithm in detail. Section 4 reports experimental results and discussion. Section 5 concludes the study and outlines future research directions.

2. Literature Review

2.1. Train Scheduling

The train scheduling problem has been extensively proven to be NP-hard [10,11]. Early research predominantly focused on constructing conflict-free space–time trajectories for trains on single or multi-track lines. Some papers did not explicitly differentiate between freight and passenger trains and implicitly included freight train scheduling in their problem formulation [12–15]. Other papers explicitly addressed the freight train scheduling problem [6,16–22]. Jovanović and Harker [16] developed the SCAN I decision-support system for tactical freight train scheduling, and Kraay and Harker [17] proposed a real-time freight train scheduling model linking tactical plans with line dispatching. While these contributions laid the methodological foundation, particularly in space–time network modeling, they implicitly assumed that once a train path is laid out in the timetable, it can be fully realized in practice. However, a series of questions remain unanswered: which specific freight should each train carry, where should the empty cars for loading come from, and how should the empty cars generated after unloading be redistributed? These are precisely the issues that dynamic railcar flow routing needs to address. Addressing these questions is particularly necessary in countries with strict train operation requirements, because the allocation of car flow directly determines the size of the trains to be operated, which, in turn, determines whether the timetable can be realized in actual operations.

Although some scholars have considered delays in the delivery of shipments when scheduling trains, implicitly considering the coupling between railcars and trains [6], they assume that sufficient empty railcars are always available for loading, and, thus, empty railcar allocation decisions are not embedded within the model. In practice, empty railcar repositioning constitutes a substantial component of daily railway operations. Unlike loaded railcars, empty railcars have no fixed flow directions, which necessitates holistic decision-making that jointly considers freight demand and the time and locations at which empty railcars are released. Accordingly, the integrated optimization of train scheduling and railcar flow routing for both loaded and empty railcars represents a critical research gap that demands attention.

2.2. Train Rescheduling Under Disruptions

When unexpected events disrupt railway operations, dispatchers must rapidly adjust the pre-planned timetable to restore feasibility. A rich body of literature has explored measures including retiming [23], reordering [24], canceling [25,26], adding [27,28], rerouting [27,29], and flexible stopping [30,31]. A common feature of these studies is their focus on adjusting macro-level timetable parameters. However, most of these model architectures were developed for passenger railways and are not directly transferable to freight operations. First, on lines shared by both passenger and freight trains, passenger trains are given higher operational priority, so freight train rescheduling is rigidly constrained by passenger train timetables. Second, unlike passenger operations, where boarding, alighting, and transferring are executed by passengers themselves, freight operations require railway authorities to organize loading, transportation, transshipment, and unloading.

Consequently, practical constraints such as transshipment time requirements and empty railcar supply must be incorporated into the rescheduling model.

Some studies have addressed freight train operations under disruptions. Haque, et al. [32] developed a rolling-horizon mixed-integer linear programming framework for the real-time integrated rescheduling of freight services and track assignment. Wang, et al. [33] focused on the problem of coordinated rescheduling of train timetable and crew scheme in the presence of disruptions on a double-track passenger–freight collinear railway. However, these studies primarily focus on optimizing the utilization of infrastructure resources and crew scheduling when rescheduling trains. Qu and He [7] developed a time–space network model and an improved A* algorithm to predict and control station traffic congestion under emergency conditions, considering the redistribution of dynamic railcar flows. Nevertheless, their model assumes that the train timetable remains fixed and only adjusts railcar flow routing results. In essence, this approach merely modifies train composition without adjusting train paths in the timetable.

Therefore, a critical research gap remains: no model jointly integrates train rescheduling and railcar flow rerouting under disruptions, notwithstanding their tight interdependence in real-world operations. Rescheduling trains without reallocating their constituent railcars may fail to adequately ensure transportation efficiency and, at the same time, may produce infeasible timetables that do not satisfy the required train marshaling constraints.

2.3. Research Comparison

From the perspective of optimization objectives, the literature on train rescheduling can be categorized into customer-centric and operator-centric approaches. The former aims to minimize the impact on customers, such as travel delays and missed connections, while the latter focuses on reducing operational costs. In the operator-centric category, Ghaemi, et al. [34] developed a MILP model for the optimal short-turning of trains during complete blockages, which determines the optimal station and timing for short-turning affected trains while considering traffic interaction on both sides of the disruption. Altazin, et al. [35] proposed a multi-objective optimization–simulation approach for real-time rescheduling in dense railway systems, optimizing recovery time, passenger service quality, and the number of operational decisions simultaneously. In the customer-centric category, Corman, et al. [36] developed microscopic passenger-centric models with decomposition-based heuristics and min-cost flow lower bounds. Dollevoet and Huisman [37] developed an iterative heuristic for large-scale delay management that accounts for passenger rerouting behavior by iteratively updating classical model parameters. Besides focusing on mitigating the impact of plan adjustments on customers, Majumder et al. [38] further proposed a data-driven framework using machine learning and rule-based techniques to quantify railway service quality, offering a complementary perspective for evaluating rescheduling outcomes.

Our paper considers both perspectives by simultaneously optimizing operational costs, plan deviation, and freight transportation efficiency. Table 1 compares our paper with related publications, categorizing them as operator-centric, customer-centric, or both. It can be found that our paper extends previous research in the following aspects:

(1) The formulated model incorporates two decisions, adjusting the space–time routes of both freight trains and railcars, an issue that no reviewed study jointly optimizes under disruptions.
(2) Most studies have only considered a single scenario, such as station disruptions, track or segment blockage, and train delays. Our paper designs multiple scenarios of unexpected events in the case study, including scenarios that are unique to freight

operations, such as changes in transportation demand, thereby demonstrating the scalability of the proposed method across different types of disturbances.

Table 1. Summary of relevant studies.

Publication	Model Structure	Timetable Adjustment	Railcar Routing	Objectives	Scenarios Considered in the Case	Solution Algorithm
Veelenturf, Kidd, Cacchiani, Kroon and Toth [29]	ILP	√		Minimize train cancellations and delays	A segment is completely blocked, a track is blocked	CPLEX
Zhan, Kroon, Veelenturf and Wagenaar [25]	MILP	√		Minimize train cancellations and deviations	A track is blocked	CPLEX + Rolling horizon
Ghaemi, Cats and Goverde [34]	MILP	√		Minimize train cancellations and delays	A station is disrupted	GUROBI
Zhu and Goverde [38]	MILP	√		Minimize train cancellations and deviations	A segment is completely blocked	GUROBI+ Rolling horizon
Sato, et al. [39]	MIP	√		Minimize the positive difference between the inconvenience the customers suffer in a rescheduled timetable and the original timetable	Train delay	GUROBI
Dollevoet and Huisman [37]	ILP	√		Minimize customers' arrival times and deviations from the macroscopic timetable	Train delay	An iterative optimization framework
Corman, D'Ariano, Marra, Pacciarelli and Sama [36]	MILP	√		Minimize customers' travel time	Train delay	Heuristic approach
Zhu and Goverde [40]	MILP	√		Minimize generalized travel times of customers	A segment is completely blocked	Adapted fix-and-Optimize algorithm
Binder, Maknoon and Bierlaire [27]	ILP	√		Minimize customer inconvenience, train operational costs, and deviations (cancellations, reroutings, delays, and the cost of adding an emergency train)	A segment is completely blocked	CPLEX + ε constraint
Altazin, et al. [41]	ILP	√		Minimize the recovery time, the number of skipped stops, the waiting time of customers, delays, and the number of delayed events	Train delay	CPLEX
Qu and He [7]	ILP		√	Minimize railcar travel time, operational costs	A station is congested	CPLEX
Zhan, Wong, Shang, Peng, Xie and Lo [8]	ILP	√		Minimize general travel cost for the customers and operational costs for the railroad company	A segment is completely blocked	CPLEX + ADMM
This publication	MILP	√	√	Minimize railcar travel time, operational costs, and deviations from the original plan	Train delays, transportation demand changes, and a segment is completely blocked	GUROBI + ε constraint

3. Materials and Methods

3.1. Problem Description

3.1.1. Dynamic Railcar Flow Routing

Dynamic railcar flow routing is the process of assembling railcars into trains for efficient transportation. The railcar flows in the railroad network consist of both loaded and empty railcar flows. Loaded railcar flows correspond to the shipment requirements of shippers. Loaded railcar flows need to go through various operations during the whole transportation process. As shown in Figure 1, after being formed at the loading station, the loaded railcars are transported to neighboring technical stations (referred to as 'marshalling yard' and 'local station' in North America) using local trains. Subsequently, the railcars are transported to the neighboring technical station of the unloading station, during which transit at other technical stations may be required. Finally, local trains are used to transport loaded railcars to the unloading station for unloading. Alternatively, dedicated (or unit) trains can be operated directly when there is a high volume of flow between the loading and unloading stations, eliminating the need for railcar transits. In this paper, only large loading stations and technical stations are considered, and traffic from the remaining stations is assumed to be consolidated to adjacent technical stations.

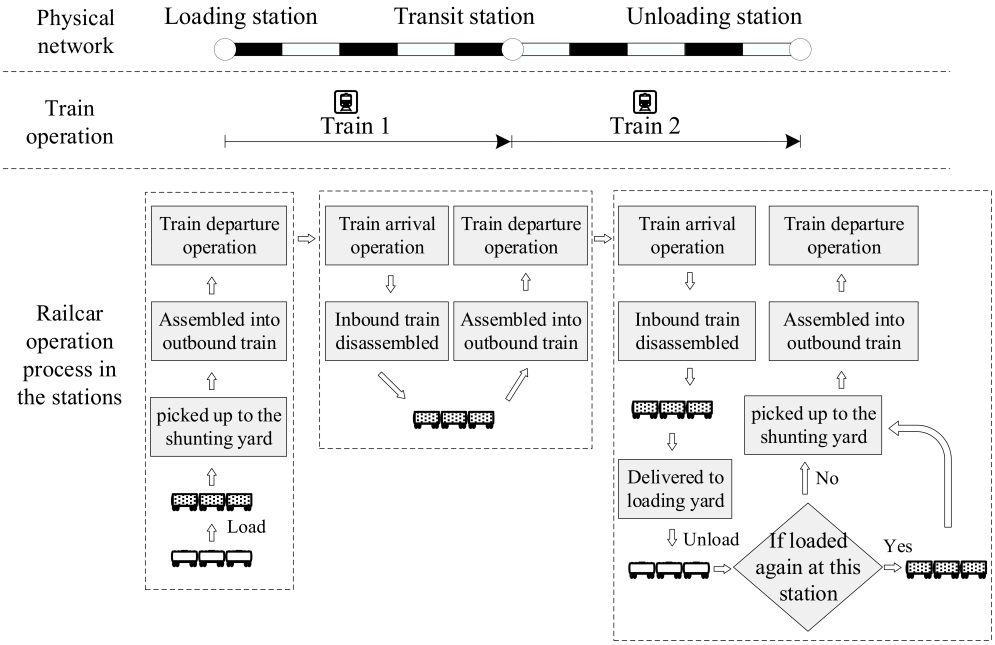


Figure 1. Railcar turnover process.

The ideal scenario is for the loaded railcars to be unloaded upon arrival at their destination and then reloaded at the same station, thereby avoiding the need for additional empty railcars to be transported. However, the number of loading and unloading railcars at each station is unbalanced. As a result, the railroad corporation has to transport empty railcars to other stations, leading to the generation of empty railcar flows. The objective of dynamic railcar flow routing is to maximize the transportation efficiency of loaded railcar flows while simultaneously minimizing the running cost of empty railcar flows.

3.1.2. Freight Train Scheduling Based on the Basic Train Timetable

In China, a critical technical document called the basic train timetable is designed based on predicted demands. The positions of train paths in the timetable are already determined, and the timetable is a feasible plan because it takes into account headway restrictions, ensuring no conflicts between train paths. However, for a freight train to

operate, it must meet certain criteria regarding weight or length. Because actual demands may differ from predicted demands, not all train paths are selected to operate trains if there is a lack of sufficient railcar flow. In such cases, dispatchers need to make decisions to formulate daily freight train operation plans by analyzing the situation. The decisions dispatchers need to make include:

(1) Selecting train paths: Based on current transportation demand and railcar distribution on the railroad network, dispatchers need to determine which train paths will be used to operate trains.
(2) Establishing connection relationships between train paths: If there is a connection relationship between two train paths, it means that they are utilized by the same train. This step allows dispatchers to determine the trajectory of each train.
(3) Distribute railcars to the trains: While determining the space–time routes of trains planned to be operated, the dispatcher needs to decide which railcars will be transported by each train. This decision indirectly creates a transportation scheme for each railcar.

To illustrate this, we provide an example in Figure 2. The figure shows six available train paths. Assume that each train can carry a maximum of 60 railcars. The dispatchers have the following information regarding transportation demand:

- There are 30 railcars each from Station A to Station B and from Station A to Station D, which have been loaded before time t1 and are waiting for departure.
- There are 30 railcars from Station B to Station D, which will be loaded after time t2 and meet the conditions for departure by time t3.

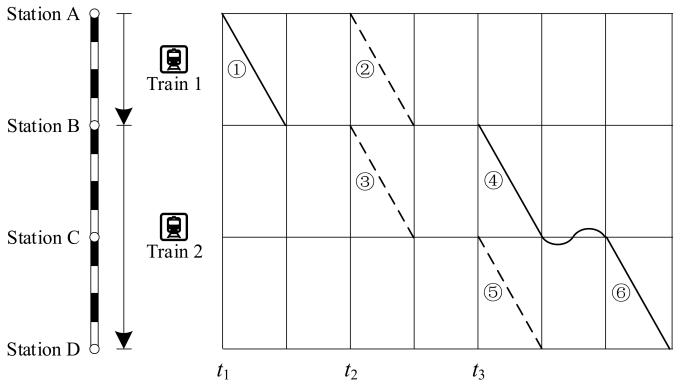


Figure 2. Freight train operation plan.

Based on the space–time distribution of the dynamic railcar flows, the dispatcher can make the following possible decisions:

- Operate Train 1 by selecting Train Path ① to transport 60 loaded railcars of A–B and A–D.
- Operate Train 2 by selecting Train Paths ④ and ⑥ and establishing a connection relationship between them to transport 60 loaded railcars of A–D and B–D.

From this decision, it is clear that the railcars of A–D will first be transported to Station B in Train 1, along with railcars of A–B. After Train 1 is disassembled, the railcars will be assembled into Train 2 together with railcars of B–D subsequently.

3.1.3. Freight Train Rescheduling

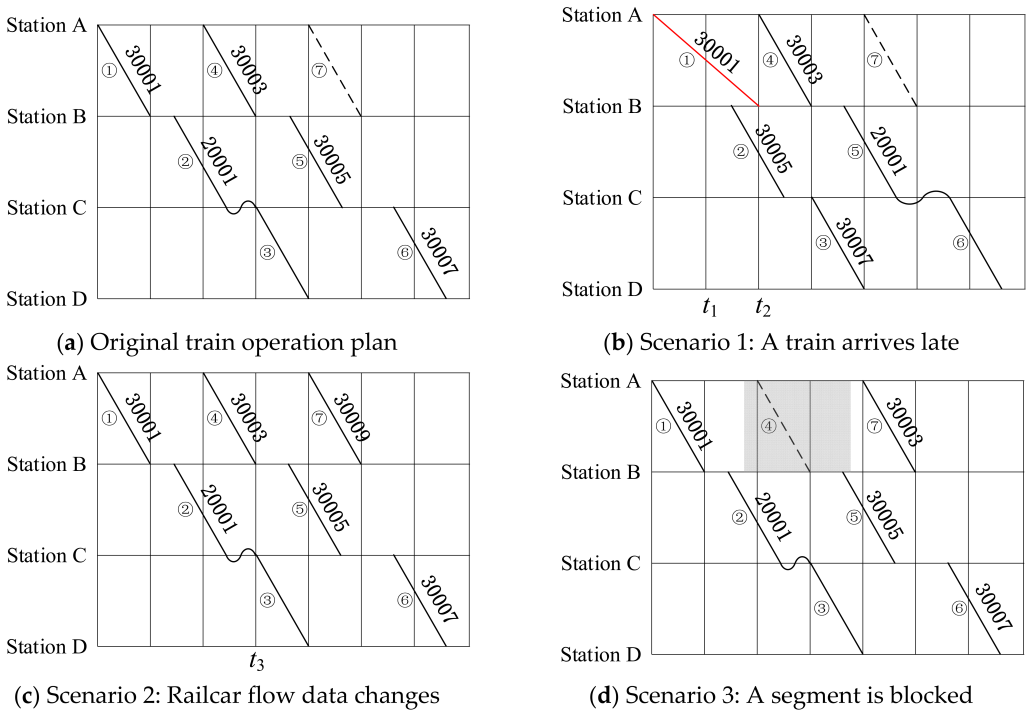
In a normal situation, trains usually run according to the predetermined plan. However, unexpected events can disrupt train operations, requiring immediate and efficient rescheduling of trains and organizing dynamic railcar flows to ensure orderly daily opera-

tions. The following are the types of unexpected events that may necessitate temporary train rescheduling:

(1) Natural disasters (e.g., earthquakes, floods, mudslides) or adverse weather conditions (e.g., hail, thunderstorms).
(2) Track blockage caused by accidents or temporary repair construction.
(3) Temporary dwelling of freight trains at stations to rescue emergency patients or ensure the safety of special trains.
(4) Station operations being disrupted, preventing trains from departing or arriving on time.
(5) Trains arriving late due to improper commands from dispatchers.
(6) Malfunctioning of railroad infrastructure.
(7) Inaccurate or temporary changes in dynamic railcar flow data.

These unexpected events can result in trains being early, late, canceled, or added, thereby affecting the execution of the original train operation plan. When such events occur, dispatchers must immediately reschedule the trains. The rescheduling decisions involve: (1) reselecting the train paths from the basic train timetable, (2) redefining the connection relationship between train paths, and (3) redefining the content of the railcar flow to be carried by each train.

Figure 3 is an example to describe the rescheduling process. The original train operation plan is presented in Table 2. The railcar flows in the railroad network consist of the following: (1) F1: 30 loaded railcars from Station A to Station B; (2) F2: 30 loaded railcars from Station A to Station D; (3) F3: 30 loaded railcars from Station B to Station D; (4) F4: 60 loaded railcars from Station A to Station B; (5) F5: 60 loaded railcars from Station B to Station C; and (6) F6: 60 loaded railcars from Station C to Station D.



(**a**) Original train operation plan

(**b**) Scenario 1: A train arrives late

(**c**) Scenario 2: Railcar flow data changes

(**d**) Scenario 3: A segment is blocked

Figure 3. Freight train rescheduling under unexpected events.

Table 2. Original freight train operation plan.

Train	Train Path Selection	Railcar Flow Content
30001	①	F1, F2
20001	②, ③	F2, F3
30003	④	F4
30005	⑤	F5
30007	⑥	F6

(1) Scenario 1: Train 30001 arrives late

Assume that Train 30001 is scheduled to arrive at Station B at time t1, but, due to unexpected conditions, it will arrive late at time t2. As a result, railcar flow F2 cannot be transferred to Train 20001 due to insufficient transfer time. The plan can be adjusted as shown in Table 3.

Table 3. Adjusted freight train operation plan in Scenario 1.

Train	Train Path Selection	Railcar Flow Content
30001	①	F1, F2
20001	⑤, ⑥	F2, F3
30003	④	F4
30005	②	F5
30007	③	F6

(2) Scenario 2: Railcar volume from A to B changes

Assuming that 60 additional railcars (A, B) are temporarily loaded at Station A at time t3, this railcar flow is defined as F7. To avoid F7 staying too long at Station A, the plan can be adjusted by adding Train 30009 (using Train Path ⑦) to transport F7.

(3) Scenario 3: Segment blockage occurs between A and B

Assume that a blockage occurred in the segment between Station A and Station B (as shown in the shaded part of Figure 3d). Train 30003 could not be operated as planned. In this case, Train 30003 can be adjusted to run along Train Path ⑦.

3.2. Model Formulation

To achieve the integrated optimization of dynamic railcar flow routing and real-time freight train rescheduling under unexpected disruptions, this study constructs a dual-layer space–time network consisting of a railcar layer and a service layer. The proposed dual-layer framework independently characterizes the spatiotemporal movement characteristics of railcar flows and freight trains, where the definitions of various network arcs inherently incorporate practical time-dimensional operation constraints, including railcar transfer time, loading and unloading time, and train dwelling time at stations. On this basis, targeted arc cost functions are defined corresponding to the multi-objective optimization goals of the system. Relying on the established dual-layer space–time network architecture, an integrated optimization model is further formulated to optimize and adjust the train operation plan.

3.2.1. Assumptions and Notations

(1) Train capacity is solely determined by the number of railcars it can accommodate. Train capacity is theoretically constrained by both gross traction weight and total train length. For simplification, the number of railcars in a consist serves as the primary operational criterion for determining whether a train meets its marshaling requirements

for departure. The proposed parameter can be readily adjusted to accommodate the specific operational rules of different railway systems in various countries.

(2) Different railcars within the same loaded railcar flow can be allocated to different trains. In this study, railcars sharing the same origin and destination and having the same transportation status at the beginning of the planning horizon are defined as belonging to the same railcar flow. Because shippers are generally concerned only with the timely arrival of their shipments rather than the specific train services used, the flow can be disaggregated without compromising service commitments.

(3) There is no distinction between types of empty railcars. In practice, empty railcars are available in various types, such as boxcars, flatcars, and hoppers, and loading specific goods requires appropriate car-type matching. Because the present study does not consider commodity types, car-type differentiation is not incorporated.

(4) The duration of certain operations at stations is measured as an average time when constructing the space–time network. In practice, station operation times, such as railcar transfer, loading and unloading, are not fixed and may vary due to workload and yard conditions. To facilitate parameter specification, this study adopts average values for simplification.

(5) The basic framework of the train timetable remains unchanged when adjusting the train operation plan. This study is set in a mixed-traffic railway system where passenger and freight trains share the same lines. To minimize the impact on passenger services, the basic timetable skeleton, specifically the number of train paths in each section, is assumed to remain fixed during rescheduling. This assumption is consistent with actual dispatching practice in China, as the basic timetable is already designed as a full-capacity graph that maximizes the utilization of line capacity.

The notations that were used in the space–time network construction and model formulation are listed in Appendix A.

3.2.2. The Space–Time Graph

(1) Service layer

Based on the physical railroad network and the train paths in the basic train timetable, various types of arcs representing all possible train movements are defined. Each station n is divided into two nodes: ARRIVAL node i_n^{arr} and DEPARTURE node i_n^{dep}. To illustrate these service-layer arcs, a simple example with two trains and three stations is shown in Figure 4.

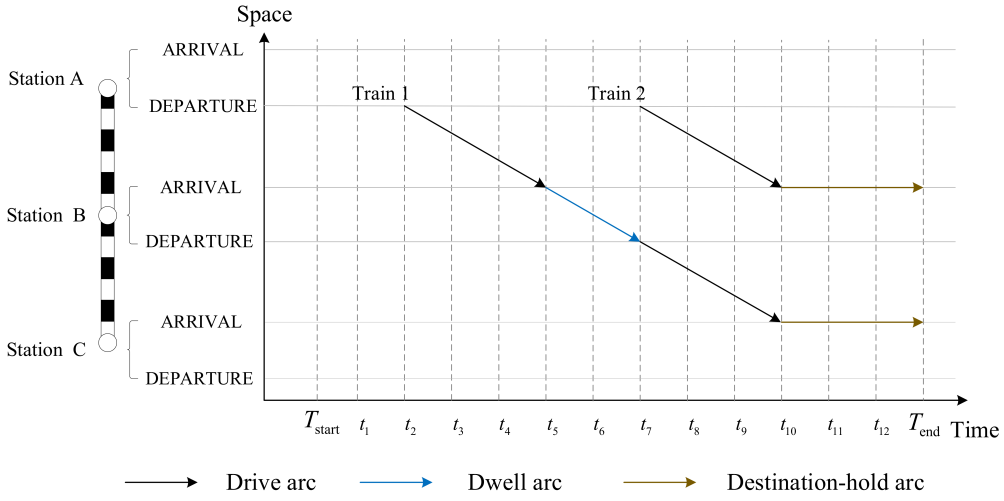


Figure 4. Service-layer space–time graph.

Drive arcs correspond to train paths in the basic train timetable. They are given by the set $L_V = \{(i,j,t,s)|i = i_m^{dep}, j = i_n^{arr}, T_{start} \le t \le T_{end}\}$. m and n represent the origin and destination stations of a train path, respectively. T_{start} and T_{end} represent the start and end of the planning horizon, respectively.

Dwell arcs represent a train stopping at a station and leaving the station within the planning horizon. A dwell arc connects the end point of a drive arc and the start point of another drive arc. They are given by the set $L_{WB} = \{(i,j,t,s)|i = i_n^{arr}, j = i_n^{dep}, s - t < T_{n,1}^{transit}\}$. In particular, at stations where trains require locomotive exchange, the arcs are given by the set $L_{WB} = \{(i,j,t,s)|i = i_n^{arr}, j = i_n^{dep}, T_{n,2}^{transit} \le s - t < T_{n,1}^{transit}\}$. $T_{n,1}^{transit}(T_{n,2}^{transit})$ represents average time railcars transit with (without) resorting at the station $n \in N$.

Destination-hold arcs represent a train stopping at a station and not leaving the station within the planning horizon ($t \le T_{end}$) or indicate that a train still running at T_{end} will stop at its arrival station ($t > T_{end}$). A destination-hold arc connects the end point of a drive arc and the ARRIVAL node of its arrival station. They are given by the set $L_{TD} = \{(i,j,t,s)|i = i_n^{arr}, j = i_n^{arr}, s = T_{end}\}$.

(2) Railcar layer

Similar to the service layer, we added the time dimension to the physical railroad network to form a railcar-layer graph, as shown in Figure 5. Each station n is spatially decomposed into four nodes: ARRIVAL node i_n^{arr}, LOADING node i_n^{load}, UNLOADING node i_n^{unload}, and DEPARTURE node i_n^{dep}. All types of arcs that represent the movements of railcars are defined below.

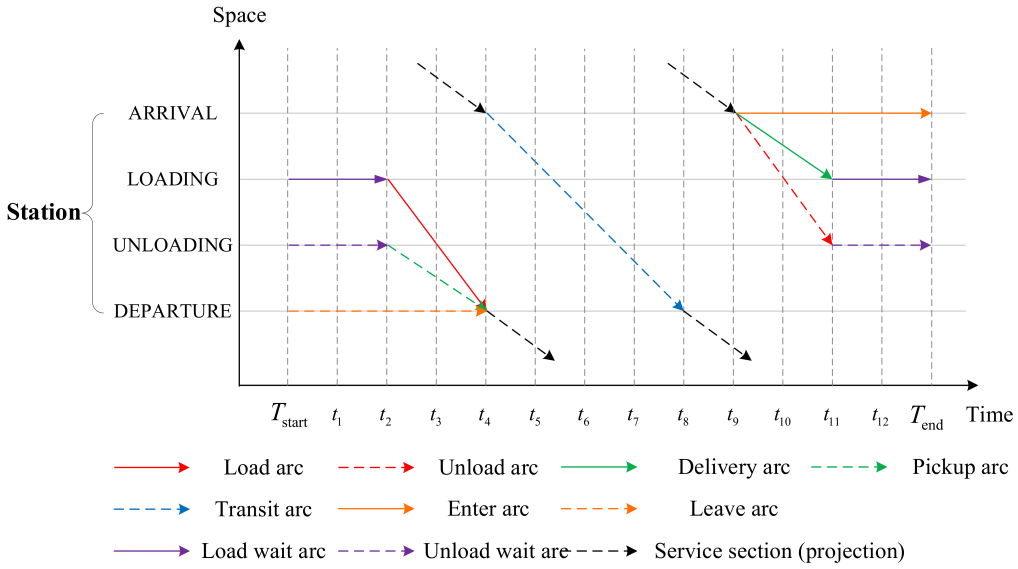


Figure 5. Railcar-layer space–time graph.

Load arcs represent shipments that are loaded, then picked up from the loading yard to the shunting yard and grouped into a train. A load arc connects the LOADING node of a station and the start point of a drive arc. They are given by the set $L_Z = \{(i,j,t,s)|i = i_n^{load}, j = i_n^{dep}, s - t = T_n^{load} + T_n^{takeout} + T_n^{assemble}\}$. T_n^{load}, $T_n^{takeout}$, and $T_n^{assemble}$ represent the average loading time, the average transfer time from the loading yard to the shunting yard, and the sum of train assembling time and departure technical operation time at station n, respectively. The sum of these three components represents the total time elapsed from the commencement of loading to the departure of the train from the station.

Unload arcs represent loaded railcars that are delivered to the unloading area and unloaded after the train they attached is disassembled. An unload arc connects the end

point of a drive arc and the station's UNLOADING node. They are given by the set $L_{\mathrm{X}} = \{(i,j,t,s)|i = i_n^{\mathrm{arr}}, j = i_n^{\mathrm{unload}}, s - t = T_n^{\mathrm{disassemble}} + T_n^{\mathrm{placein}} + T_n^{\mathrm{unload}}\}$. $T_n^{\mathrm{disassemble}}$, T_n^{placein}, and T_n^{unload} represent the sum of a train's arrival technical operation time and disassembling operation time, the average time for delivering railcars from the shunting yard to the loading yard, and the average time for unloading loaded railcars at station n, respectively. The sum of these three components represents the total time elapsed from the train's arrival to the completion of unloading.

Delivery arcs represent empty railcars that are delivered to the loading area after the train they attached is disassembled. A delivery arc connects a drive arc's end point and the station's LOADING node. They are given by the set $L_{\mathrm{JS}} = \{(i,j,t,s)|i = i_n^{\mathrm{arr}}, j = i_n^{\mathrm{load}}, s - t = T_n^{\mathrm{disassemble}} + T_n^{\mathrm{placein}}\}$.

Pickup arcs model empty railcars that are picked up from the unloading area to the shunting yard and grouped into a train. A pickup arc connects the UNLOADING node of a station and the start point of a drive arc. They are given by the set $L_{\mathrm{QB}} = \{(i,j,t,s)|i = i_n^{\mathrm{unload}}, j = i_n^{\mathrm{dep}}, s - t = T_n^{\mathrm{takeout}} + T_n^{\mathrm{assemble}}\}$.

Dual load arcs represent railcars that have been unloaded and are waiting to be loaded again. A dual load arc connects the end point of an unload arc and the adjacent start point of a load arc. They are given by the set $L_{\mathrm{ET}} = \{(i,j,t,s)|i = i_n^{\mathrm{unload}}, j = i_n^{\mathrm{load}}, s \geq t\}$.

Transit arcs model railcars transferring from one train to another one in a station, with a minimal transfer time. A transit arc connects the end point of a drive arc and the start point of another driver arc. They are given by the set $L_{\mathrm{B}} = \{(i,j,t,s)|i = i_n^{\mathrm{arr}}, j = i_n^{\mathrm{dep}}, s - t \geq T_{n,1}^{\mathrm{transit}}\}$.

Enter arcs model railcars stopping at the station until T_{end} after the train it attached is disassembled. An enter arc connects the end point of a drive arc and the ARRIVAL node of the same station. They are given by the set $L_{\mathrm{DW}} = \{(i,j,t,s)|i = i_n^{\mathrm{arr}}, j = i_n^{\mathrm{arr}}, s = T_{\mathrm{end}}\}$.

Leave arcs represent railcars that are stopping at the shunting yard and are grouped into a train. A leave arc connects the DEPART node of a station and the start point of a drive arc. They are given by the set $L_{\mathrm{CW}} = \{(i,j,t,s)|i = i_n^{\mathrm{dep}}, j = i_n^{\mathrm{dep}}, s - t \geq T_n^{\mathrm{assemble}}\}$.

Load wait arcs represent shipments that are waiting to be loaded or empty railcars that are waiting at the loading area. A load wait arc connects the LOADING nodes of the same station. They are given by the set $L_{\mathrm{ZW}} = \{(i,j,t,s)|i = i_n^{\mathrm{load}}, j = i_n^{\mathrm{load}}, T_{\mathrm{start}} \leq t < s \leq T_{\mathrm{end}}\}$.

Unload wait arcs represent loaded railcars that have already been unloaded or empty railcars that are waiting at the unloading area. An unload wait arc connects the UNLOADING nodes of the same station. They are given by the set $L_{\mathrm{XW}} = \{(i,j,t,s)|i = i_n^{\mathrm{unload}}, j = i_n^{\mathrm{unload}}, T_{\mathrm{start}} \leq t < s \leq T_{\mathrm{end}}\}$.

Super arcs represent a failure to load shipments that were required to be loaded according the loading plan. They are given by the set $L_{\mathrm{S}} = \{(i,j,t,s)|i = i_n^{\mathrm{load}}, j = i_n^{\mathrm{load}}, t = T_{\mathrm{start}}, s = T_{\mathrm{end}}\}$.

(3) Rescheduling graph

The rescheduling graph $G(V^*, L^*)$ can be regarded as a subgraph of the complete graph $G(V, L)$. When freight trains are being rescheduled, certain drive arcs in the set $\{(i,j,t,s)|(i,j,t,s) \in L_{\mathrm{V}}, t < T_{\mathrm{reschedule}}, s > T_{\mathrm{reschedule}}\}$ may not be planned for the distribution of railcars according to the original plan. $T_{\mathrm{reschedule}}$ denotes the time point at which rescheduling decisions are made. Therefore, these drive arcs and all other arcs connected to them can be removed from the rescheduling graph. Additionally, there are certain arcs that cannot be utilized in unexpected events. In such cases, it is necessary to analyze the specific situation and remove these arcs accordingly. For example, if a segment is completely blocked, it is evident that trains cannot pass through it. Therefore, the drive arcs that are not allowed to be selected, along with other arcs connected to them, can be deleted from the graph. Another example is when a train arrives late, causing some railcar flows to be

unable to be transferred to another train within the minimum transit time constraint. In this scenario, transit arcs involving these railcars that violate the minimum transit time constraint can be removed from the graph.

3.2.3. Cost for Loaded Railcar Flows Using the Arcs

This paper abstracts the problem of transporting loaded railcars into a multi-commodity flow problem. In order to find suitable space–time routes for each loaded railcar flow, the origins and destinations of the flows within the space–time network must be established (see Appendix B). Furthermore, the cost of each arc must be appropriately defined based on the optimization objective.

A loaded railcar flow refers to a group of loaded railcars that share the same destination station and have the same status at the start time of the planning horizon. The dispatchers aim to minimize the time it takes for these flows to reach their destinations. Therefore, when determining the arc cost, penalties are considered for loaded railcar flows that remain at stations. It is assumed that the penalty cost is related to the time, and the cost conversion coefficient is denoted as ξ. The cost definition process for some arcs is described in detail below:

(1) Enter arcs and destination-hold arcs $(i, j, t, s) \in L_{\mathrm{DW}} \cup L_{\mathrm{TD}}$: If a loaded railcar flow is assigned to the arc, the flow arrives at the station with the train and stays there until the end of the planning horizon. The total dwell time at the stations is $\left[(t - (t_f + T^{f,n}_{\mathrm{travel}})\right] + (T_{\mathrm{end}} - t) = T_{\mathrm{end}} - t_f - T^{f,n}_{\mathrm{travel}}$. The arc cost is $\xi(T_{\mathrm{end}} - t_f - T^{f,n}_{\mathrm{travel}})$. t_f denotes the temporal origin of railcar flow f in the space–time network. $T^{f,n}_{\mathrm{travel}}$ denotes the total in-transit travel time of flow f from its origin to the station n.

(2) Unload arcs $(i, j, t, s) \in L_{\mathrm{X}}$: If a loaded railcar flow is assigned to the arc, the flow arrives at the station with the train at t and completes the unloading operation. The total dwell time at the stations is $\left[(t - (t_f + T^{f,n}_{\mathrm{travel}})\right] + (s - t) = s - t_f - T^{f,n}_{\mathrm{travel}}$. The arc cost is $\xi(s - t_f - T^{f,n}_{\mathrm{travel}})$.

(3) Leave arcs $(i, j, t, s) \in L_{\mathrm{CW}}$ $(s = T_{\mathrm{end}})$: If a loaded railcar flow is assigned to the arc, the flow stays at the station during the planning horizon. The total dwell time at the stations is $T_{\mathrm{end}} - T_{\mathrm{start}}$. The arc cost is $\xi(T_{\mathrm{end}} - T_{\mathrm{start}})$.

(4) Super arcs $(i, j, t, s) \in L_{\mathrm{S}}$: If $f \in F'$ is assigned to the arc, the corresponding shipments are not loaded during the planning horizon. F' denotes the set of railcar flows awaiting loading. The total dwell time at the stations is $T_{\mathrm{end}} - T_{\mathrm{start}}$. The arc cost is $\xi(T_{\mathrm{end}} - T_{\mathrm{start}})$.

(5) Drive arcs $(i, j, t, s) \in L_{\mathrm{V}}$: In the making of the original plan, it is assumed that the loaded railcar flows need to be transported according to the prescribed physical route, so some drive arcs that violate the physical route regulations cannot be selected by the loaded railcar flows. These arcs are added to $L_f^{\mathrm{V,forbidden}}$, and their costs are set to infinity (Z).

(6) Pickup arcs, delivery arcs and dual load arcs $(i, j, t, s) \in L_{\mathrm{QB}} \cup L_{\mathrm{JS}} \cup L_{\mathrm{ET}}$: These arcs can only be selected by empty railcars, so the arc cost is set to infinity (Z).

Figure 6 provides an example illustrating the process of searching for space–time routes for loaded railcar flows. Assuming a planning horizon from 0:00 to 24:00 and travel times of 6 h for both A–B and B–C, Table 4 presents the information on the loaded railcar flows within the railroad network. Table 5 lists several feasible routes for the loaded railcar flows. By applying the defined arc cost, the cost for each space–time route was calculated, enabling the identification of the optimal feasible route.

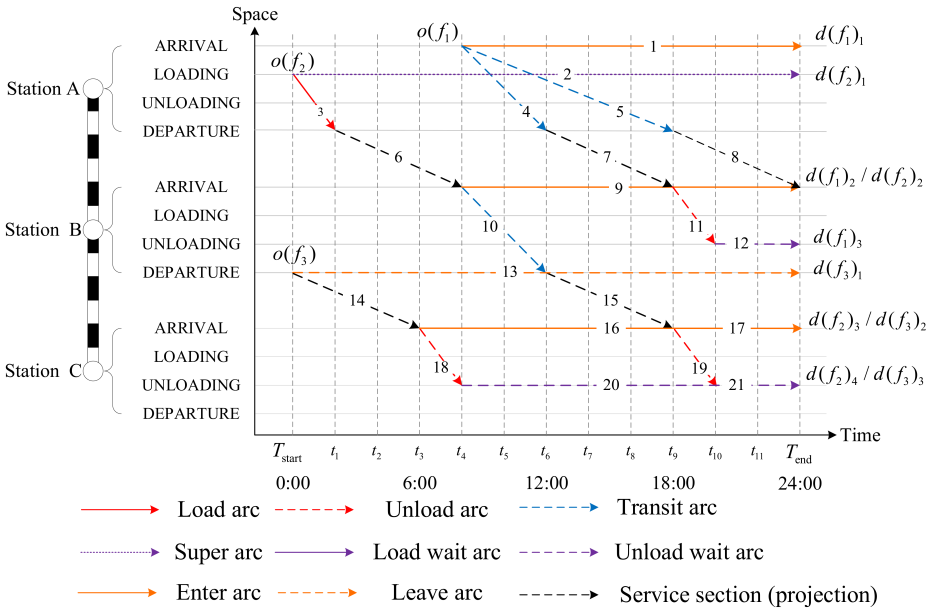


Figure 6. An illustrative example of loaded railcars' space–time route.

Table 4. Specific information of the loaded railcar flows in Figure 6.

Loaded Railcar Flow Index	Initial Status	Origin Node	Unloading Station	N_f	$T^{f,n}_{\text{travel}}$, $n \in N_f$(h)
f_1	Running with a train and will arrive at Station A at t_4	$o(f_1) = (i^{\text{arr}}_{\text{A}}, t_4)$	B	A, B	0, 6
f_2	Waiting to be loaded at Station A	$o(f_2) = (i^{\text{load}}_{\text{A}}, T_{\text{start}})$	C	A, B, C	0, 6, 12
f_3	Already been loaded and is waiting to depart from Station B	$o(f_3) = (i^{\text{dep}}_{\text{B}}, T_{\text{start}})$	C	B, C	0, 6

Table 5. Space–time routes of the loaded railcar flows in Figure 6.

Loaded Railcar Flow Index	Feasible Space–Time Routes	Corresponding Destination in the Space–Time Network	Total Dwell Time (h)	Optimal Route
f_1	Route (1): 1 Route (2): 5 → 8 Route (3): 4 → 7 → 11 → 12	$d(f_1)_1 = (i^{\text{arr}}_{\text{A}}, T_{\text{end}})$ $d(f_1)_2 = (i^{\text{arr}}_{\text{B}}, T_{\text{end}})$ $d(f_1)_3 = (i^{\text{unload}}_{\text{B}}, T_{\text{end}})$	$T_{\text{end}} - t_4 - T^{1,\text{A}}_{\text{travel}} = 24 - 8 - 0 = 16$ $T_{\text{end}} - t_4 - T^{1,\text{B}}_{\text{travel}} = 24 - 8 - 6 = 10$ $t_{10} - t_4 - T^{1,\text{B}}_{\text{travel}} = 20 - 8 - 6 = 6$	Route (3)
f_2	Route (1): 2 Route (2): 3 → 6 → 9 Route (3): 3 → 6 → 10 → 15 → 17 Route (4): 3 → 6 → 10 → 15 → 19 → 21	$d(f_2)_1 = (i^{\text{load}}_{\text{A}}, T_{\text{end}})$ $d(f_2)_2 = (i^{\text{arr}}_{\text{B}}, T_{\text{end}})$ $d(f_2)_3 = (i^{\text{arr}}_{\text{C}}, T_{\text{end}})$ $d(f_2)_4 = (i^{\text{unload}}_{\text{C}}, T_{\text{end}})$	$T_{\text{end}} - T_{\text{start}} = 24$ $T_{\text{end}} - T_{\text{start}} - T^{2,\text{B}}_{\text{travel}} = 24 - 0 - 6 = 18$ $T_{\text{end}} - T_{\text{start}} - T^{2,\text{C}}_{\text{travel}} = 24 - 0 - 12 = 12$ $t_{10} - T_{\text{start}} - T^{2,\text{C}}_{\text{travel}} = 20 - 0 - 12 = 8$	Route (4)
f_3	Route (1): 13 Route (2):14 → 16 Route (3): 14 → 18 → 20	$d(f_3)_1 = (i^{\text{dep}}_{\text{B}}, T_{\text{end}})$ $d(f_3)_2 = (i^{\text{arr}}_{\text{C}}, T_{\text{end}})$ $d(f_3)_3 = (i^{\text{unload}}_{\text{C}}, T_{\text{end}})$	$T_{\text{end}} - T_{\text{start}} = 24$ $T_{\text{end}} - T_{\text{start}} - T^{3,\text{C}}_{\text{travel}} = 24 - 0 - 6 = 18$ $t_4 - T_{\text{start}} - T^{3,\text{C}}_{\text{travel}} = 8 - 0 - 6 = 2$	Route (3)

3.2.4. Cost for Empty Railcars Using the Arcs

For empty railcars, running costs only occur when they are allocated to the drive arcs. A conversion coefficient, denoted as γ, is introduced to quantify these costs ($\gamma(s-t)$). However, the unload arcs, load arcs and super arcs $(i, j, t, s) \in L_{\text{X}} \cup L_{\text{Z}} \cup L_{\text{S}}$ can only be utilized by loaded railcar flows. Therefore, the cost associated with these arcs is defined as infinity (Z).

3.2.5. Model

$$\min Z_S = \sum_f \sum_{(i,j,t,s)\in L^*} q_f \cdot c^f_{i,j,t,s} \cdot x^f_{i,j,t,s} \tag{1}$$

$$\min Z_O = c_{\text{train}} \cdot \sum_{(i,j,t,s)\in L_V \cap L^*} y_{i,j,t,s} + \sum_{(i,j,t,s)\in L^*} c^{\text{empty}}_{i,j,t,s} \cdot z_{i,j,t,s} + \sum_{n\in N_e} c^{\text{empty}}_{\text{punish}} (q^{\text{empty}}_n - \sum_{(i,j,t,s)\in L_{V,n}\cap L^*} z_{i,j,t,s}) \tag{2}$$

$$\min Z_D = \sum_{(i,j,t,s)\in L_V \cap L^*} \left| y_{i,j,t,s} - \overline{y}_{i,j,t,s} \right| + \sum_{(i,j,t,s)\in L^* \cap \{(i,j,t,s)|\overline{w}_{i,j,t,s}=0\}} w_{i,j,t,s} + \sum_{(i,j,t,s)\in L^* \cap \{(i,j,t,s)|\overline{v}_{i,j,t,s}=0\}} v_{i,j,t,s} \tag{3}$$

From the perspective of shippers, it is desirable to have their shipments delivered as quickly as possible. Meanwhile, the railroad company aims to minimize operational costs. To minimize disruptions to daily operations, the railroad company also seeks to minimize deviations from the original freight train operation plan. Therefore, three objective functions are defined in Equations (1)–(3).

Equation (1): The travel time cost of shipments Z_S is quantified by the travel time of loaded railcars. q_f denotes the number of railcars associated with flow f; $c^f_{i,j,t,s}$ denotes the unit cost for f using arc $(i,j,t,s) \in L^*$; L^* denotes the set of arcs in the rescheduling space–time graph; and $x^f_{i,j,t,s}$ is a decision variable that indicates the proportion of flow f assigned to arc (i,j,t,s), $x^f_{i,j,t,s} \in [0,1]$.

Equation (2): The operational costs Z_O are measured using three metrics. In Equation (2), the first sum represents the fixed cost of train operations, where c_{train} denotes the fixed cost of selecting a train path in the basic train timetable and $y_{i,j,t,s}$ is a binary decision variable that equals 1 if arc (i,j,t,s) is selected and 0 otherwise. The second sum represents the transportation cost of empty railcars, where $c^{\text{empty}}_{i,j,t,s}$ denotes the unit cost for empty railcars using arc (i,j,t,s) and decision variable $z_{i,j,t,s}$ denotes the number of empty railcars assigned to arc (i,j,t,s). The third sum represents the penalty cost for failing to deliver sufficient empty railcars to other railroad companies as planned, where $c^{\text{empty}}_{\text{punish}}$ denotes the unit penalty cost, q^{empty}_n represents the required number of empty railcars to be delivered, and $L_{V,n}$ denotes the set of arcs passing through the boundary station $n \in N_e$.

Equation (3): The deviation cost Z_D represents the penalty for deviations from the original plan. In Equation (3), the first sum aims to minimize changes to the train path selection scheme, where $\overline{y}_{i,j,t,s}$ is a given binary parameter that equals 1 if arc (i,j,t,s) is used in the original plan. The second and third sums aim to avoid adding humping tasks and assembling tasks at unplanned time points, respectively, where $w_{i,j,t,s}$ is a binary decision variable that equals 1 if the train using arc $(i,j,t,s) \in L$ is disassembled after arriving and $v_{i,j,t,s}$ is a binary decision variable that equals 1 if the train using arc (i,j,t,s) is assembled before departing.

$$\sum_{(i,j,t,s)\in L^*|(j,s)=o(f)} x^f_{i,j,t,s} = 0 \quad \forall f \in F \tag{4}$$

$$\sum_{(j,i,s,t)\in L^*|(j,s)=o(f)} x^f_{j,i,s,t} = 1 \quad \forall f \in F \tag{5}$$

$$\sum_{(i,j,t,s)\in L^*|(j,s)\in D(f)} x^f_{i,j,t,s} = 1 \quad \forall f \in F \tag{6}$$

$$\sum_{(j,i,s,t)\in L^*|(j,s)\in D(f)} x^f_{j,i,s,t} = 0 \quad \forall f \in F \tag{7}$$

$$\sum_{(i,j,t,s)\in L^*} x^f_{i,j,t,s} - \sum_{(j,i,s,t)\in L^*} x^f_{j,i,s,t} = 0 \quad \forall f \in F, \forall (j,s) \in V \backslash \{o(f), D(f)\} \tag{8}$$

Constraints (4)–(8) are the loaded railcar flow conservation constraints, which ensure that each loaded railcar flow f can find feasible space–time routes between its origin and destination.

$$\sum_{f\in F} q_f \cdot x^f_{i,j,t,s} + z_{i,j,t,s} \le q^{\max}_{i,j,t,s} \cdot y_{i,j,t,s} \quad \forall (i,j,t,s) \in L_{\text{train}} \cap L^* \tag{9}$$

Constraint (9) ensures that the total quantity of railcars assigned to a train does not exceed its capacity. $q^{\max}_{i,j,t,s}$ denotes the maximum capacity of arc (i,j,t,s).

$$\sum_{(i',j',t',s')\in \Phi_1(i,j,t,s)} \Big(\sum_{f\in F} q_f \cdot x^f_{i',j',t',s'} + z_{i',j',t',s'}\Big) \le q^{\max}_{i,j,t,s} \cdot w_{i,j,t,s} \quad \forall (i,j,t,s) \in L_{\text{V}} \cap L^*, T_{\text{start}} < s < T_{\text{end}} \tag{10}$$

$$\sum_{(i',j',t',s')\in \Phi_2(i,j,t,s)} \Big(\sum_{f\in F} q_f \cdot x^f_{i',j',t',s'} + z_{i',j',t',s'}\Big) \le q^{\max}_{i,j,t,s} \cdot v_{i,j,t,s} \quad \forall (i,j,t,s) \in L_{\text{V}} \cap L^*, T_{\text{start}} < t < T_{\text{end}} \tag{11}$$

Constraints (10) and (11) are coupling constraints. Constraint (10) states that railcars can only be distributed to the arcs in $\Phi_1(i,j,t,s)$ when $w_{i,j,t,s} = 1$. Similarly, Constraint (11) states that railcars can only be distributed to the arcs in $\Phi_2(i,j,t,s)$ when $v_{i,j,t,s} = 1$. Sets $\Phi_1(i,j,t,s)$ and $\Phi_2(i,j,t,s)$ consist of railcar-level arcs connected to the end point and start point of arc $(i,j,t,s) \in L_{\text{V}}$, respectively. These two constraints ensure that railcar flows can be transferred from the service layer to the railcar layer only after the train corresponding to arc (i,j,t,s) is disassembled and can be transferred from the railcar layer to the service layer only before the train corresponding to arc (i,j,t,s) is assembled. In other words, the consist composition of a train must remain unchanged from the completion of its assembly to its final disassembly.

$$\sum y_{i',j',t',s'} = 1 - w_{i,j,t,s} \quad \forall (i',j',t',s') \in \Pi_1(i,j,t,s), (i,j,t,s) \in L_{\text{V}} \cap L^*, T_{\text{start}} < s < T_{\text{end}} \tag{12}$$

$$\sum y_{i',j',t',s'} = 1 - v_{i,j,t,s} \quad \forall (i',j',t',s') \in \Pi_2(i,j,t,s), (i,j,t,s) \in L_{\text{V}} \cap L^*, T_{\text{start}} < t < T_{\text{end}} \tag{13}$$

Constraint (12) denotes that if $w_{i,j,t,s} = 0$, railcars can only be distributed to one arc in $\Pi_1(i,j,t,s)$, which ensures that any train that is not disassembled after arriving at a station can only choose one train path to continue its journey or remain at the station. Constraint (13) ensures that multiple trains that are not disassembled after arriving at a station cannot choose the same train path to continue their journey. $\Pi_1(i,j,t,s)$ and $\Pi_2(i,j,t,s)$ consist of service-level arcs connected to the end point and start point of drive arc $(i,j,t,s) \in L_{\text{V}}$, respectively.

$$w_{i,j,t,s} \le y_{i,j,t,s} \quad \forall (i,j,t,s) \in L_{\text{V}} \cap L^*, T_{\text{start}} < s < T_{\text{end}} \tag{14}$$

$$v_{i,j,t,s} \le y_{i,j,t,s} \quad \forall (i,j,t,s) \in L_{\text{V}} \cap L^*, T_{\text{start}} < t < T_{\text{end}} \tag{15}$$

Constraints (14) and (15) denote that if a drive arc is not selected, both $w_{i,j,t,s}$ and $v_{i,j,t,s}$ are equal to 0, which ensures that train disassembly and marshaling operations are possible only when the corresponding train path is utilized.

$$\sum_{(i,j,t,s)\in (L_{\text{S}} \cup L_{\text{Z}}) \cap L^*} x^f_{i,j,t,s} = 1 \quad \forall f \in F' \tag{16}$$

Constraint (16) indicates that the railcar flow waiting to be loaded $f \in F'$ must be assigned to either load arcs or the super arc, which ensures that shipments can only be transported after being loaded.

$$\sum_{(i,j,t,s)\in L_{\mathrm{V},n}\cap L^*} z_{i,j,t,s} \le q_n^{\mathrm{empty}} \quad \forall n \in N_{\mathrm{e}} \tag{17}$$

Constraint (17) indicates that the volume of empty railcars delivered to other railway companies through boundary stations must not exceed the volume specified by the superior orders.

$$z_{i,j,t,s} = q_{i,j,t,s}^{\mathrm{empty}} \quad \forall (i,j,t,s) \in L^{\mathrm{empty}} \cap L^* \tag{18}$$

At the beginning of the planning horizon, empty railcars exist in the network, either running on trains or dwelling at stations. Constraint (18) assigns initial empty railcar flow volumes to the corresponding arcs L^{empty} as the initial input to the network. $q_{i,j,t,s}^{\mathrm{empty}}$ denotes the empty railcar flow volume on arc (i,j,t,s).

$$\sum_{(i,j,t,s)\in L^*} z_{i,j,t,s} = \sum_{(j,i,s,t)\in L^*} z_{j,i,s,t} \quad \forall (i,t) \in S(L_{\mathrm{V}}) \cup E(L_{\mathrm{V}}) \cup E(L_{\mathrm{JS}}) \cup S(L_{\mathrm{QB}}) \tag{19}$$

Constraint (19) ensures that the inflow of empty railcars equals the outflow of empty railcars at certain nodes. $S(L)$ and $E(L)$ denote the collections of nodes that serve as the start and end points of the arcs in L, respectively.

$$\sum_{(j,i,s,t)\in(L_{\mathrm{ET}}\cup L_{\mathrm{LW}})\cap L^*} z_{(j,i,s,t)} = \sum_{(i,j,t,s)\in L_{\mathrm{LW}}\cap L^*} z_{i,j,t,s} + \sum_{f\in F'} \sum_{(i,j,t,s)\in L_{\mathrm{Z}}\cap L^*} q_f \cdot x_{i,j,t,s}^f \quad \forall (i,t) \in S(L_{\mathrm{Z}}) \tag{20}$$

$$\sum_{f\in F} \sum_{(j,i,s,t)\in L_{\mathrm{X}}\cap L^*} q_f \cdot x_{j,i,s,t}^f = \sum_{(i,j,t,s)\in(L_{\mathrm{ET}}\cup L_{\mathrm{QB}}\cup L_{\mathrm{XW}})\cap L^*} z_{i,j,t,s} \quad \forall (i,t) \in E(L_{\mathrm{X}}) \tag{21}$$

The loaded railcars are converted to empty railcars at the end points of the unload arcs, and some empty railcars are converted to loaded railcars at the start points of the load arcs. Constraints (20) and (21) make sure that the inflow of railcars equals the outflow of railcars at these nodes.

$$x_{i,j,t,s}^f = \overline{x}_{i,j,t,s}^f \quad \forall (i,j,t,s) \in L_{\mathrm{train}} \cap L^*, t \le T_{\mathrm{reschedule}} \tag{22}$$

$$z_{i,j,t,s} = \overline{z}_{i,j,t,s} \quad \forall (i,j,t,s) \in L_{\mathrm{train}} \cap L^*, t \le T_{\mathrm{reschedule}} \tag{23}$$

Constraints (22) to (23) ensure that the distribution of railcars complies with the original plan before any rescheduling decision is made. $\overline{x}_{i,j,t,s}^f$ denotes the proportion of f distributed to arc (i,j,t,s) according to the original plan. $\overline{z}_{i,j,t,s}$ denotes the volume of empty railcars distributed to arc (i,j,t,s) according to the original plan.

$$x_{i,j,t,s}^f \in [0,1] \quad \forall f \in F, \forall (i,j,t,s) \in L^* \tag{24}$$

$$y_{i,j,t,s} \in \{0,1\} \quad \forall (i,j,t,s) \in L_{\mathrm{train}} \cap L^* \tag{25}$$

$$z_{i,j,t,s} \in Z^+ \quad \forall (i,j,t,s) \in L^* \tag{26}$$

$$w_{i,j,t,s} \in \{0,1\} \quad \forall (i,j,t,s) \in L_{\mathrm{V}} \cap L^* \tag{27}$$

$$v_{i,j,t,s} \in \{0,1\} \quad \forall (i,j,t,s) \in L_{\mathrm{V}} \cap L^* \tag{28}$$

Constraints (24)–(28) define the domains of the variables.

To solve the model using mathematical optimization solvers, it is necessary to linearize the objective function (3). This can be achieved by introducing an intermediate variable

$u_{i,j,t,s}$ to replace the first sum in the objective function. Additionally, four constraints (30) to (33) are added to ensure linearization. As a result, the objective function (3) can be transformed into the linearized form (29).

$$\min Z_D = \sum_{(i,j,t,s)\in L_V \cap L^*} u_{i,j,t,s} + \sum_{(i,j,t,s)\in L^* \cap \{(i,j,t,s)|\overline{w}_{i,j,t,s}=0\}} w_{i,j,t,s} + \sum_{(i,j,t,s)\in L^* \cap \{(i,j,t,s)|\overline{v}_{i,j,t,s}=0\}} v_{i,j,t,s} \quad (29)$$

$$u_{i,j,t,s} \le y_{i,j,t,s} - \overline{y}_{i,j,t,s} \quad \forall (i,j,t,s) \in L^* \cap \{(i,j,t,s)|\overline{y}_{i,j,t,s} = 1\} \quad (30)$$

$$u_{i,j,t,s} \ge 2(y_{i,j,t,s} - \overline{y}_{i,j,t,s}) - 1 \quad \forall (i,j,t,s) \in L^* \cap \{(i,j,t,s)|\overline{y}_{i,j,t,s} = 1\} \quad (31)$$

$$u_{i,j,t,s} \le \overline{y}_{i,j,t,s} - y_{i,j,t,s} \quad \forall (i,j,t,s) \in L^* \cap \{(i,j,t,s)|\overline{y}_{i,j,t,s} = 0\} \quad (32)$$

$$u_{i,j,t,s} \ge 2(\overline{y}_{i,j,t,s} - y_{i,j,t,s}) - 1 \quad \forall (i,j,t,s) \in L^* \cap \{(i,j,t,s)|\overline{y}_{i,j,t,s} = 0\} \quad (33)$$

3.3. A Pareto Solution Search Framework Based on the ε-Constraint Method

In multi-objective mathematical programming (MOMP), the focus is on searching for Pareto-optimal solutions rather than a single optimal solution that optimizes all objective functions simultaneously. Common methods used in solving MOMP problems include the weighting and ε-constraint methods. The weighting method involves combining different objectives into a single objective using weights. The ε-constraint method optimizes one objective function while incorporating the other objective functions as constraints.

The ε-constraint method offers several advantages over the weighting method in MOMP [42]:

(1) It can produce non-extreme efficient solutions, ultimately leading to identifying the Pareto set.
(2) It eliminates the need to scale the objective functions to a common scale before forming the weighted sum.
(3) The number of generated efficient solutions can be controlled by adjusting the number of grid points in each objective function range.

Therefore, to quantify the trade-offs between the three objective functions, the ε-constraint method is adopted. This method involves constructing a single-objective optimization model where one of the objective functions from the multi-objective planning is chosen as the objective function. An ε constraint is then added to the constraints, which restricts the upper bounds of the other objectives in the multi-objective planning. By continuously adjusting the value of ε, the upper bounds of the other multi-objective functions are changed, and the Pareto solution is obtained.

To solve the rescheduling problem, the original plan based on the complete graph (step (1) in Table 6) needs to be obtained. It is important to minimize railcar flow transportation efficiency before considering the operational costs for two reasons. Firstly, if transportation efficiency is chosen as the first objective, it would completely sacrifice customer interests, resulting in impractical and extreme solutions. Specifically, no trains would be exclusively operated to transport railcars. Additionally, prioritizing customer satisfaction is necessary in a highly competitive market.

When exploring the three-dimensional Pareto frontier of the rescheduling problem, the model is first solved with transportation time cost of shipments as the optimization objective. In subsequent steps, the upper bound of transportation time cost is determined by attaching a coefficient to $Z_S^{U,2}$ obtained in step 2.1. However, determining adjustment coefficients to cover the wide range of possible values for the deviation costs is challenging. Therefore, in step 2.2, operational costs and deviation costs are used as optimization objectives to obtain the range of the deviation costs, then various values in $[Z_D^U, Z_D^{SN}]$ are

selected as the upper bound of the deviation costs. The detailed procedure for exploring the Pareto frontier is provided in Appendix C.

Table 6. Main characteristics of the methodology to explore the Pareto frontier.

Step	Objective	Constraints	Output Value	Network
(1.1)	Z_S	(4)–(21), (24)–(28)	$Z_S^{U,1}$	$G(V, L)$
(1.2)	Z_O	(4)–(21), (24)–(28) $Z_S \leq \varepsilon_{S,1} \cdot Z_S^{U,1}$, $\varepsilon_{S,1} \in [1, 1.1]$	-	$G(V, L)$
(2.1)	Z_S	(4)–(28), (30)–(33)	$Z_S^{U,2}$	$G(V^*, L^*)$
(2.2.1)	Z_D	(4)–(28), (30)–(33) $Z_S \leq \varepsilon_{S,2} \cdot Z_S^{U,2}$, $\varepsilon_{S,2} \in [1, 1.1]$	Z_D^U	$G(V^*, L^*)$
(2.2.2)	Z_O	(4)–(28), (30)–(33) $Z_S \leq \varepsilon_{S,2} \cdot Z_S^{U,2}$, $\varepsilon_{S,2} \in [1, 1.1]$	Z_D^{SN}	$G(V^*, L^*)$
(2.2.3)	Z_O	(4)–(28), (30)–(33) $Z_S \leq \varepsilon_{S,2} \cdot Z_S^{U,2}$, $\varepsilon_{S,2} \in [1, 1.1]$ $Z_D \leq \varepsilon_D$, $\varepsilon_D = Z_D^{SN} - (\frac{Z_D^{SN} - Z_D^U}{q^{max}}) \cdot s$ $s = 1, 2, \ldots, q^{max}$	-	$G(V^*, L^*)$

3.4. Application Procedure of the Proposed Method

The overall solution procedure for applying the proposed model and algorithm under unexpected events is depicted in Figure 7. When an unexpected event occurs, it is necessary to assess its impact on the original space–time network according to the event type and make structural adjustments if required. The model is then solved to generate a new timetable by redefining the connection relationships between train paths, while the consist composition of each train is determined based on the railcar flow assignment results. Throughout this process, the deviation of the adjusted plan from the original plan is evaluated to minimize the disruption to normal operations caused by the plan adjustment. It should be noted that the Pareto solution search framework is not intended to enumerate all Pareto solutions but rather to flexibly generate feasible adjusted plans according to the dispatcher's balancing of customer and operator interests.

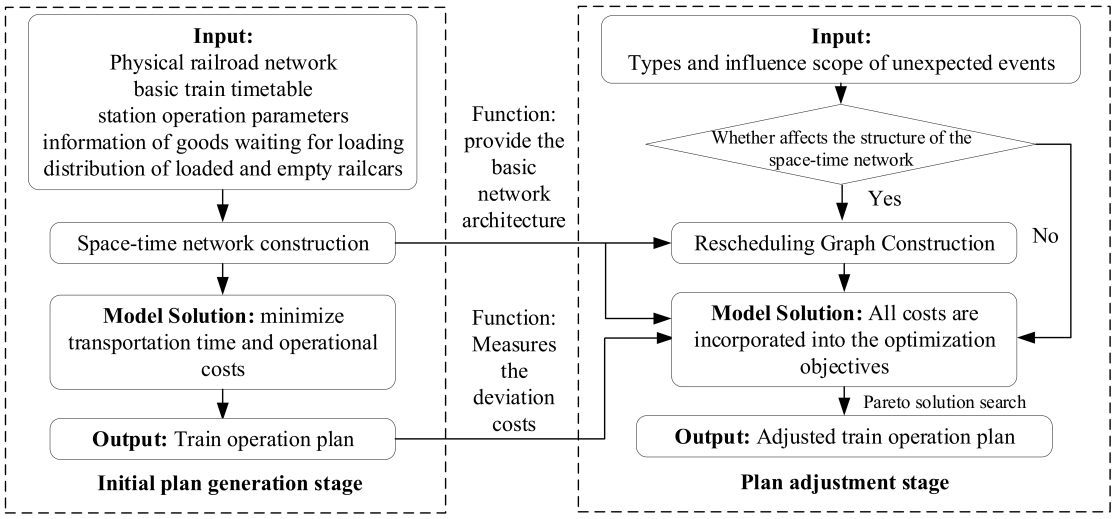


Figure 7. Methodology steps.

4. Results and Discussion

This section presents the experimental results of applying our approach to the network of a Chinese railroad company. The mathematical model is solved using Gurobi 9.1.0 on a personal computer with a 2.6 GHz Intel(R) Core(TM) i7-9750H CPU and 16 GB of RAM. In order to obtain feasible solutions efficiently, the termination condition for each model solving is set to either a 1% solution gap or a solution time of 1200 s. This is particularly important, as multiple models need to be solved to obtain a set of Pareto solutions.

4.1. Case Description

To validate our model and algorithm, tests on the Chinese railroad network were conducted, as shown in Figure 8. This network consists of 25 stations represented by circles. The original plan starts at 18:00 on a specific day, and the planning horizon covers 24 h. At the beginning of the planning horizon, there are 475 loaded railcar flows within the railroad network. The basic timetable consists of 759 train paths. Each train has a capacity of 60 railcars.

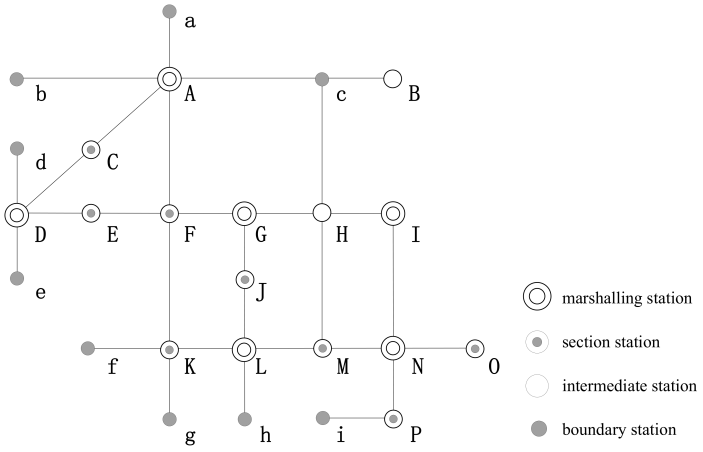


Figure 8. Topological network of a Chinese railroad company.

The unit cost of using a train path (c_{train}) is 5000, and the conversion coefficient for the running cost of empty railcars (γ) is 0.1/min. The unit penalty cost for not delivering empty railcars to other railroad companies as superior orders ($c^{\text{empty}}_{\text{punish}}$) is 300. The penalty cost conversion coefficient for loaded railcars dwelling at stations is set as follows: $\xi(f \in F \backslash F') = 2/\text{h}$, $\xi(f \in F') = 1/\text{h}$. It is important to note that the value of $\xi(f \in F \backslash F')$ is chosen to be greater than that of $\xi(f \in F')$ to ensure the efficient transportation of shipments that have already been loaded at the start of the planning horizon. In practice, the specific values of these parameters can be determined according to the preferences and requirements of the dispatchers.

Three scenarios were created to simulate unexpected events:

(1) Scenario 1: Train delay

At 24:00, the dispatcher received information about localized adverse weather conditions, which caused nine trains currently running between Station D and Station E to arrive 15 min late.

(2) Scenario 2: Transportation demand changes

At 6:00 the next day, some stations received new orders for loading from shippers. According to statistics, the transportation demand for 40 origin–destination (OD) pairs increased by five to 10 percent compared to the original level.

(3) Scenario 3: Segment blockage

At 1:00 the next day, a disruption occurred in the segment between Station A and Station F, and it was expected to last for 5 h. During this disruption, the tracks in the affected segment were unavailable.

All experimental data in this study, including railcar flows, train paths, and disruption scenarios, are generated based on real-world railway network data and are available at https://data.mendeley.com/preview/68xs5yxvc7?a=94700ca3-80b2-46c6-afdb-e473321d459d (accessed on 24 August 2026).

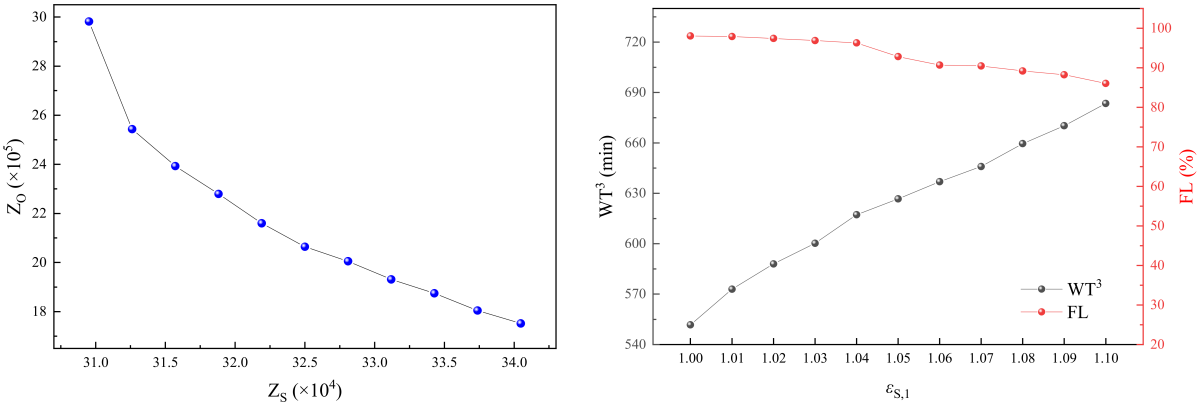
4.2. Generation of the Original Plan

Before applying the rescheduling framework, it is necessary to generate the original plan based on the complete graph, as outlined in steps (1.1) and (1.2) of Table 6. The results are presented in Table 7, which yields eleven Pareto solutions. To assess the trade-off between shipper satisfaction and operational costs, the Pareto frontier for different values of Z_S and Z_O is plotted in Figure 9a. Additionally, Figure 9b illustrates the variation in certain indicators with $\varepsilon_{S,1}$. It is observed that operational costs decrease more slowly as shipment transportation time cost increases, which indicates that more shipper satisfaction needs to be sacrificed to save on operational costs. Two indicators, WT^3 and FL in Table 7, partially reflect the quality of transportation services. When $\varepsilon_{S,1}$ exceeds 1.04, the fulfillment rate of the loading plan significantly decreases, and adjusting $\varepsilon_{S,1}$ from 1.03 to 1.04 results in a notable increase in the average waiting time of loaded railcar flows. By weighing the two optimization objectives, the solution with $\varepsilon_{S,1} = 1.03$ was selected as the original plan.

Table 7. Computational results for the original plan.

$\varepsilon_{S,1}$	Z_S	Z_O	TO	PS	WT^1 [Min]	WT^2 [Min]	WT^3 [Min]	FL [%]
1	309,523	2,982,033	406	559	237.02	689.22	551.71	98.05
1.01	312,619	2,543,499	359	481	235.22	720.59	572.99	97.91
1.02	315,713	2,392,674	345	455	238.25	740.82	587.98	97.42
1.03	318,809	2,279,516	333	433	240.59	757.46	600.28	96.90
1.04	321,904	2,159,902	316	409	239.27	782.50	617.31	96.31
1.05	325,000	2,064,391	302	394	243.97	793.91	626.67	92.84
1.06	328,095	2,005,490	297	384	251.71	805.30	636.95	90.71
1.07	331,190	1,931,302	288	369	260.21	814.58	645.99	90.49
1.08	334,285	1,874,534	278	358	262.38	833.20	659.61	89.22
1.09	337,380	1,804,313	272	345	265.15	847.24	670.23	88.24
1.1	340,476	1,751,915	264	335	267.72	865.18	683.49	86.07

Related indicators after scheduling: number of trains operated (TO), number of train paths selected (PS), loaded railcar flows' average waiting time at the stations ($f \in F \backslash F'$: WT^1, $f \in F'$: WT^2, $f \in F$: WT^3), fulfillment rate of the loading plan (FL).



(**a**) Pareto frontier for original plan

(**b**) Some indicators for different values of $\varepsilon_{S,1}$

Figure 9. Computational results for original plan.

4.3. Experimental Results and Discussion

4.3.1. Generation of Pareto-Optimal Solutions

For each scenario, the Pareto solution set is generated according to step 2 in Table 6, where the parameter q^{max} is uniformly set to 6 (if more Pareto solutions are sought, this value can be set larger as needed). The time required for step 2.1 is recorded in Table 8. This step can be accomplished quickly in all scenarios. Table 9 provides the number of feasible and Pareto-optimal solutions obtained by applying the solution framework. Most of the feasible solutions obtained are non-dominated, which demonstrates that the solution framework in this paper yields favorable results.

Table 8. The time required to complete Step (2.1).

	Scenario 1	**Scenario 2**	**Scenario 3**
CPU Time [s]	38.83	29.66	66.34

Table 9. Number of feasible and Pareto-optimal solutions.

	Scenario 1	**Scenario 2**	**Scenario 3**
Number of feasible solutions	72	76	73
Number of Pareto-optimal solutions	58	58	66

Appendix D compares several Pareto-optimal solutions of the model for different values of Z_S and Z_D, including only non-dominated and feasible solutions. The first and second columns indicate the upper bounds imposed on shipment transportation time cost and deviation from the original plan, respectively. Columns three to five give the optimal values of three objectives. Column six gives the solution time. Relevant indicators of the new plan are reported in columns seven to twelve. Columns thirteen to sixteen respectively report relevant metrics for measuring deviation from the original plan: the number of train paths newly selected, the number of train paths canceled, the number of assembling tasks added at unplanned time points, and the number of humping tasks added at unplanned time points.

Pareto-optimal solutions are represented by dots in Figure 10, which depicts a 3D scatter figure showing the three objectives. A common feature is evident in the scatterplots for the three scenarios: the operational cost and the deviation cost of most Pareto-optimal solutions are concentrated within a certain range. This makes it easier for dispatchers to quickly make decisions during the rescheduling process without solving many Pareto-optimal solutions. The primary focus can be on the size of the shipment transportation time cost.

4.3.2. Analysis of the Results

This subsection aims to offer valuable insights into the trade-offs associated with different objectives by analyzing the results of the experiments under each scenario and generalizing them to find common features. Considering the limitations of the 3D graphical visualization shown in Figure 10, we further draw subgraphs for detailed analysis.

To quantify the trade-off between the operational cost and deviation cost, the Pareto frontier for different values of shipment transportation time cost was plotted in Figure 11. The almost-vertical lines in the figure show that the operational cost can be reduced significantly with a slight initial increase in the deviation cost. However, if the deviation cost continues to increase, the reduction in the operational cost is no longer so significant. Thus, with the upper bound on shipment transportation time cost fixed, railroad companies

may consider accepting smaller changes to their original schedules to achieve greater operational cost savings. However, large adjustments to the schedules are not worth it.

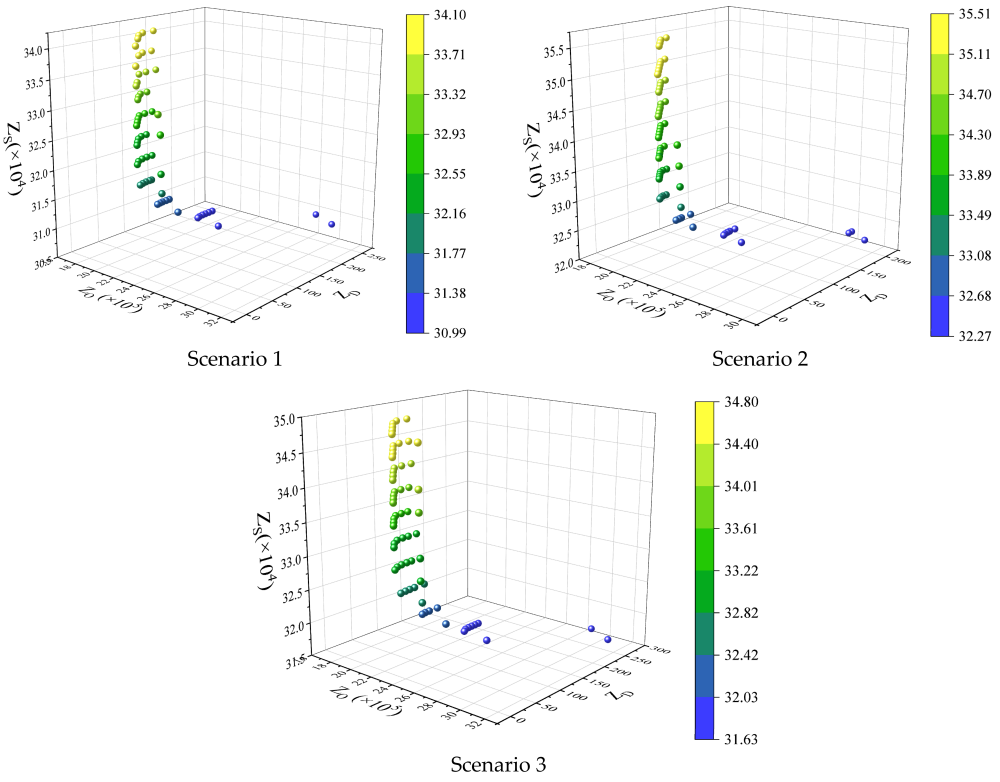


Figure 10. Pareto-optimal solutions.

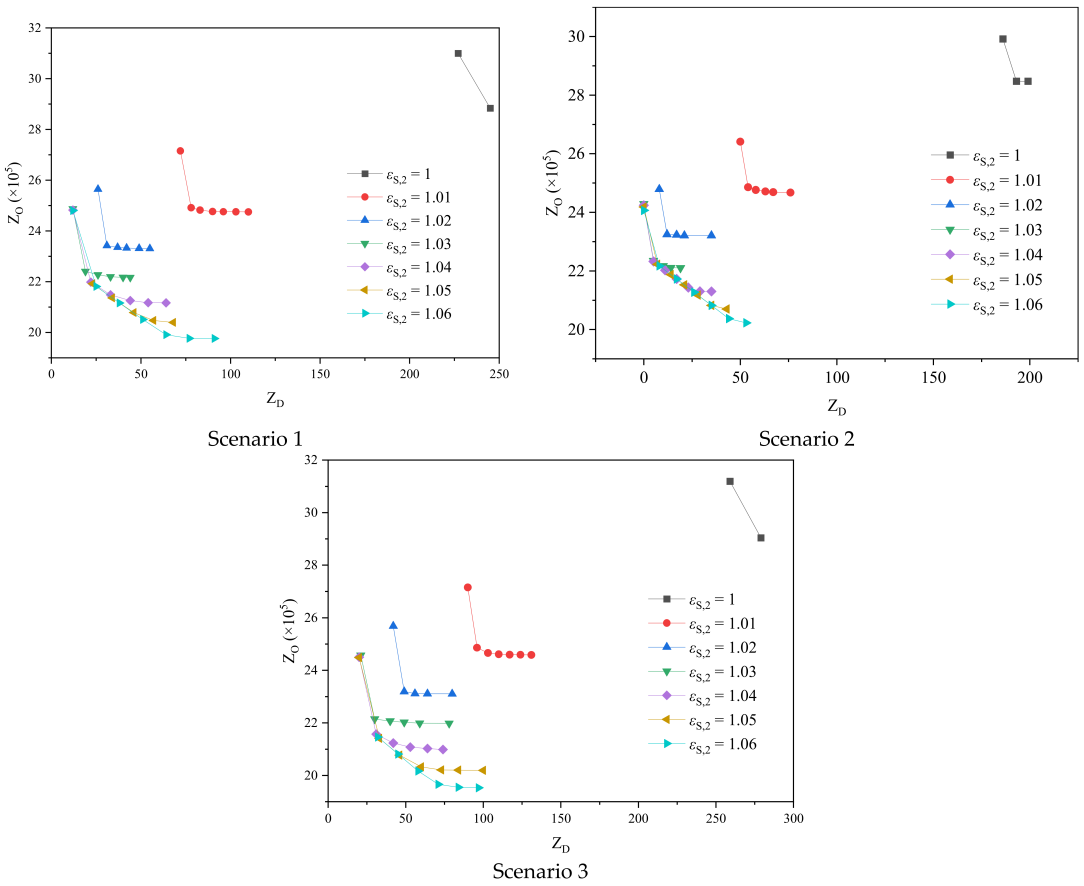


Figure 11. Trade-off between the operational cost and the deviation cost.

Next, we focus on analyzing the effect of shipment transportation time cost values on the experimental results. Figure 12 shows that the average waiting time at stations for loaded railcar flows and the loading plan fulfillment rate highly depend on the upper bound of shipment transportation time cost. In all scenarios, the overall characteristics of the changes in these two indicators can be similar to those that occurred when the original plan was generated. The growth trend of WT^3 remains stable as $\varepsilon_{S,2}$ grows, but when $\varepsilon_{S,2}$ exceeds 1.02 or 1.03, the fulfillment rate of the loading plan significantly decreases.

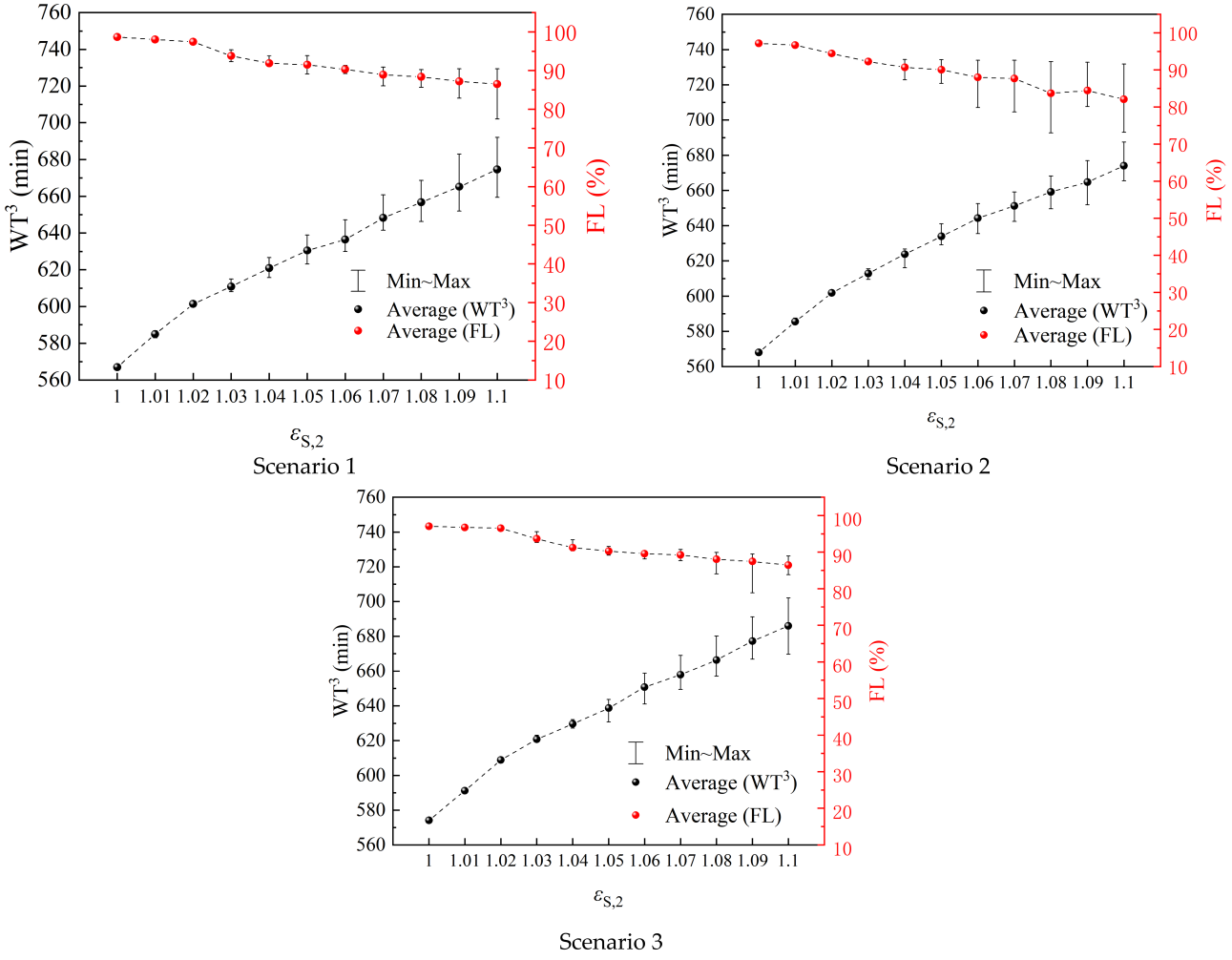


Figure 12. Some indicators for different values of $\varepsilon_{S,2}$.

Take Scenario 1 as an example: with a lower upper bound value (e.g., $\varepsilon_{S,2} = 1$), the loading plan fulfillment rate can reach up to 98.1%, and the average waiting time at stations for loaded railcar flows can decrease by as much as 42.23 min compared to the original plan. When the upper bound value is higher (e.g., $\varepsilon_{S,2} = 1.1$), the fulfillment rate of the loading plan drops to only 83.92%, and the average waiting time at stations for loaded railcar flows can increase by as much as 85.12 min compared to the original plan. This option is unsatisfactory from the shipper's perspective, but it does result in lower operational costs, with an average reduction of 36.12% compared to the case where $\varepsilon_{S,2}$ equals 1. The above analysis and description prove that transportation time cost, whether too large or too small, is more extreme and undesirable. Therefore, when formulating or adjusting the plan, railway companies should avoid unilaterally pursuing the lowest operational cost or the best service. Instead, they should adopt a moderate level of service quality to achieve an effective balance between cost and service.

Figures 13 and 14 depict the distribution of the operational cost and the deviation cost in the Pareto-optimal solution for each value of shipment transportation time cost, respectively. Figure 13 shows that in all scenarios, the Pareto values of the operational cost initially decrease significantly as shipment transportation time cost increases, and then the rate of decline slows. This pattern aligns with the Pareto frontier of the original plan. For instance, in Scenario 1, when $\varepsilon_{S,2}$ increased from 1 to 1.05, the mean value of operational cost in the Pareto solutions decreased from 29.92 $\times$ 10^5 to 20.99 $\times$ 10^5, reflecting a decrease of 29.85%. Furthermore, from 1.05 to 1.1, the average value only decreased to 19.11 $\times$ 10^5, representing a decrease of 8.93%. These research findings indicate that moderate reductions in customer satisfaction within a certain range have the potential to achieve savings in operational costs exceeding 20%.

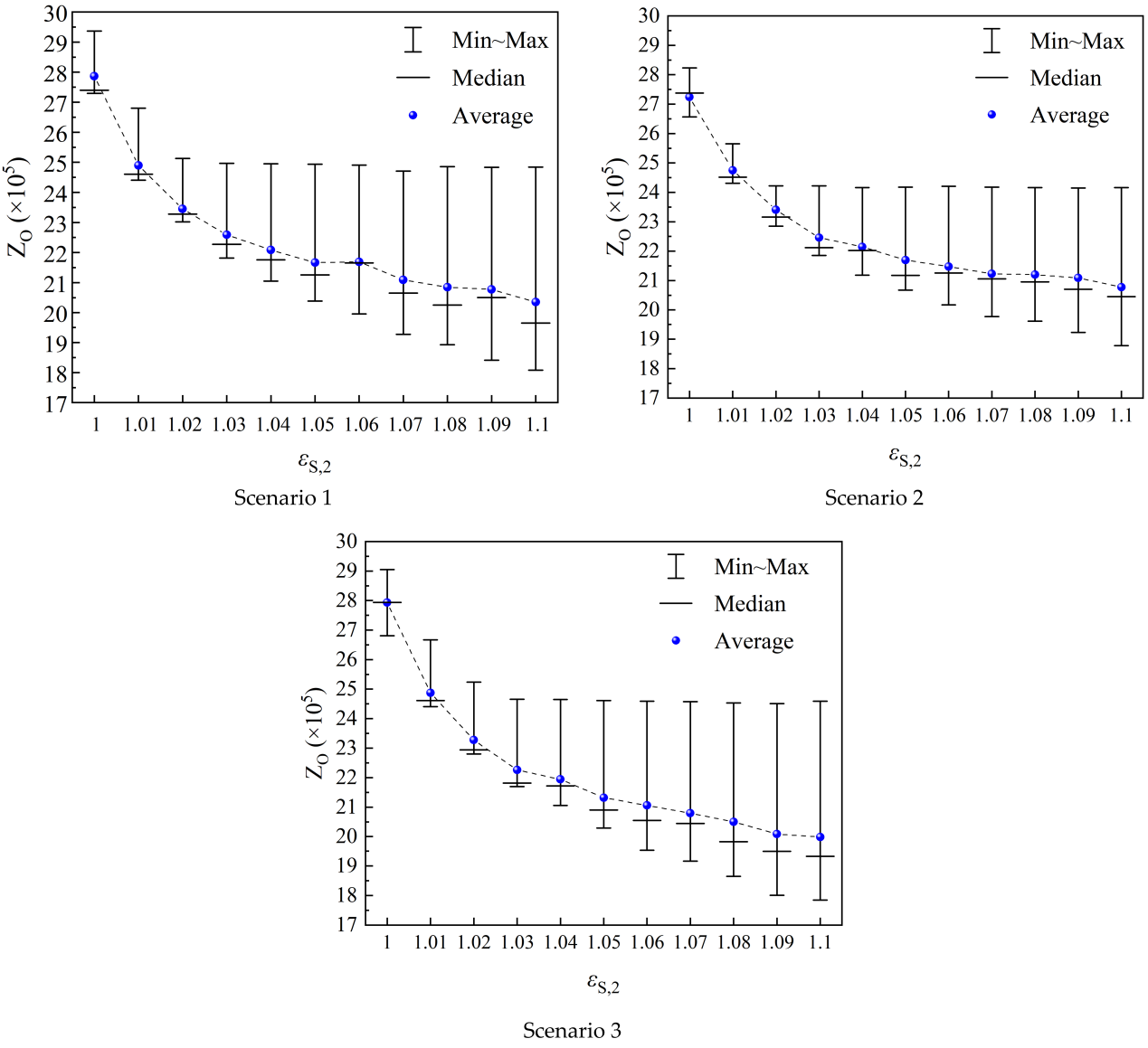


Figure 13. Z_O for different values of $\varepsilon_{S,2}$.

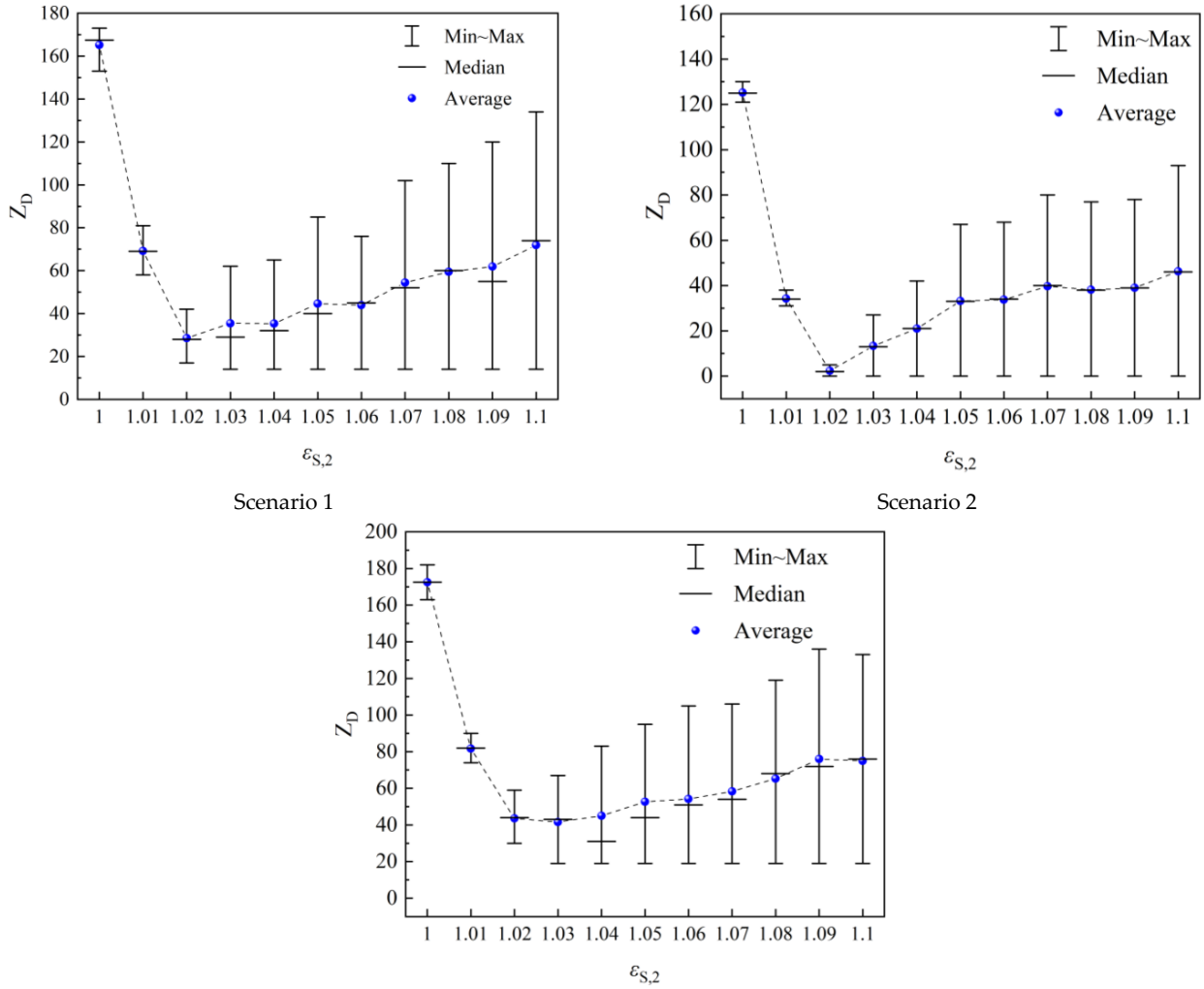


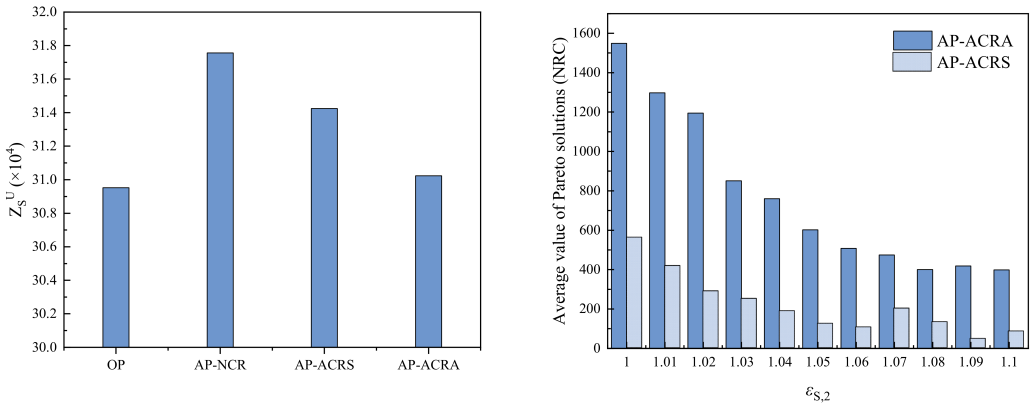
Figure 14. Z_D for different values of $\varepsilon_{S,2}$.

As depicted in Figure 14, in all scenarios, as shipment transportation time cost increases, the operational cost in the Pareto solutions initially decreases significantly overall and then gradually increases. For example, in Scenario 1, when $\varepsilon_{S,2}$ increases from 1 to 1.03, the average value of the deviation cost decreases from 236 to 29, a decrease of 87.71%. Moreover, when it increases to 1.1, the mean value increases from 29 to 85.6, instead increasing by 195.17%. These findings suggest that a modest reduction in customer satisfaction can significantly reduce deviations from the original plan when making rescheduling decisions. Too much sacrifice of customer satisfaction, on the other hand, is not particularly significant in terms of operational cost savings, and on the other hand, the degree of deviation from the plan can increase dramatically, which is not conducive to the orderliness of day-to-day work.

The above experimental results demonstrate that when adjusting the plan under unexpected disruptions, service quality, operational cost, and plan stability cannot be simultaneously optimized, which leaves dispatchers facing difficult trade-off decisions in practice. The patterns revealed by the experiments provide clear guidance: moderately reducing service quality can help control operational costs while maintaining plan stability; additionally, moderate schedule adjustments can significantly reduce costs, but when adjustments become excessively large, the marginal benefit of cost savings diminishes considerably and is no longer worthwhile.

4.3.3. Analysis of the Effects of Introducing Candidate Routes

In Scenario 3, different strategies were implemented to adjust the plan. In Figure 15a, OP means the original plan, and the other abbreviations used are explained below:



(**a**) Z_S^U for different strategies (**b**) NRC for different values of $\varepsilon_{S,2}$

Figure 15. Computational results for adding candidate physical routes.

AP-NCR: Add No Candidate Physical Routes—This strategy involves not adding any candidate physical routes when making adjustments to the plan. In other words, loaded railcars can only be transported along the predetermined physical route when adjusting the plan.

AP-ACRS: Only Add Candidate Physical Routes for Affected Loaded Railcars—This strategy focuses on adding candidate physical routes only for the loaded railcars that are directly affected by the blocked segment.

AP-ACRA: Add Candidate Physical Routes for All Loaded Railcars—This strategy involves adding candidate physical routes for all loaded railcars, regardless of whether they are affected by the blocked segment.

Candidate physical routes are alternative detours that can be activated when the primary physical route is blocked. Take Figure 16 as an example. Initially, the loaded railcar flow is planned to follow the physical route A → B → C. In this case, the railcar flow can be distributed to Train Paths 1 and 2. However, if segment B-D is blocked, the railcar flow cannot be distributed to Train Path 2. Consequently, the loaded railcar flow has to stop at Station B. To address this issue and avoid long dwell times at the stations, an alternative route A → B → C → D can be considered if it meets the requirements of candidate routes. By using Train Paths 3 and 4 in this case, the loaded railcar flow can bypass the blocked segment and continue its journey without dwelling for an extended period at the stations.

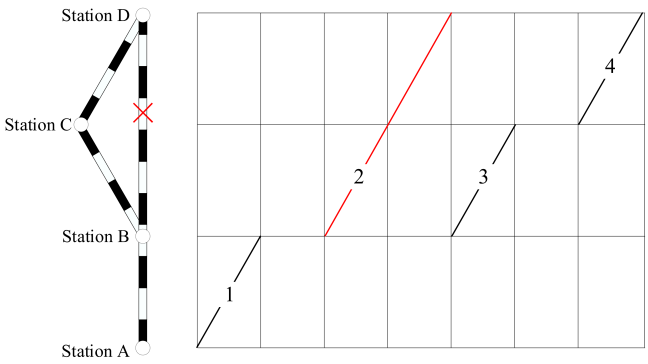


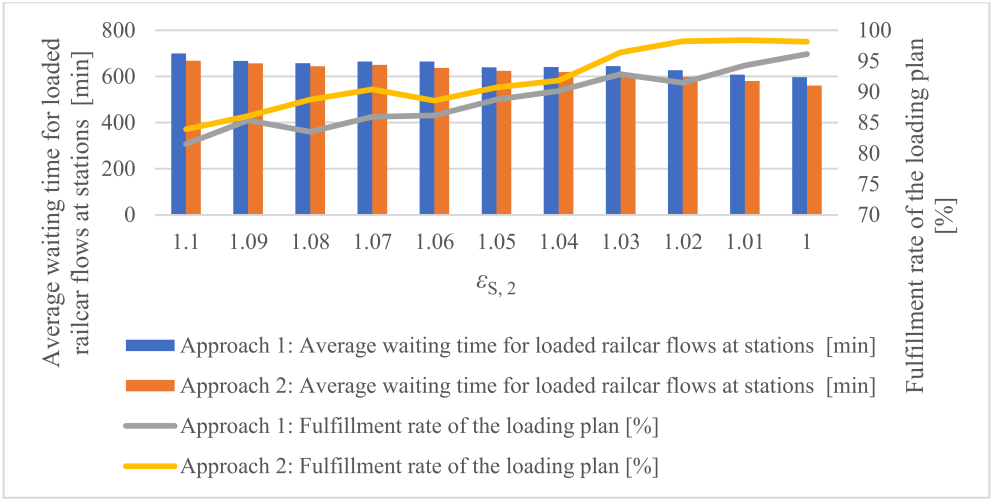
Figure 16. An illustrative example of rerouting.

In Figure 15b, NRC represents the number of loaded railcars that are reallocated to the other physical routes. The experimental findings indicate a significant decrease in shipment transportation time cost following the introduction of alternative physical routes. Furthermore, incorporating alternative routes for a larger number of loaded railcar flows can enhance the quality of transportation services more effectively. Specifically, AP-ACRA achieves a 2.3% saving in shipment travel time cost compared to AP-NCR.

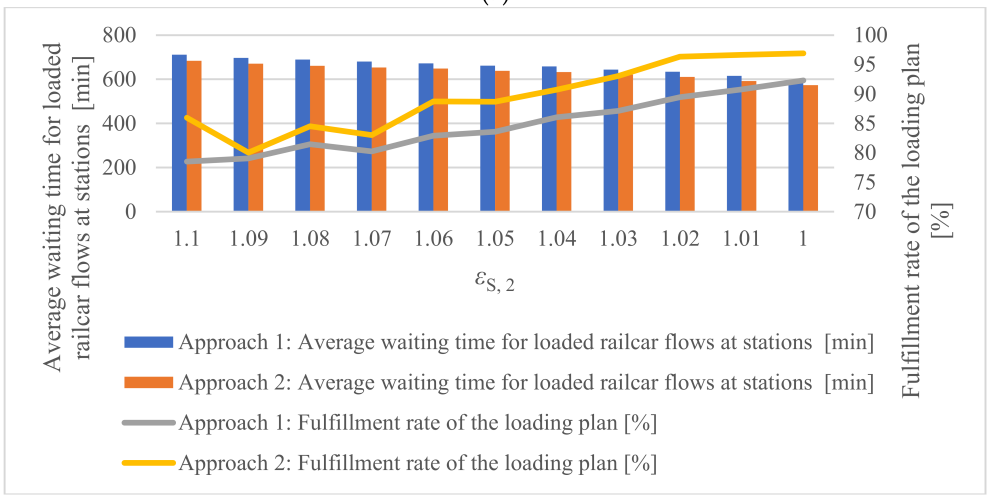
4.3.4. Performance Analyses of the Method

(1) Optimization performance

To verify the effectiveness of our method, a comparison with one baseline is conducted, as shown in Figure 17a–c. Approach 1 represents the strategy that cancels disrupted trains directly without timetable adjustments and then reassigns the railcar flows. Approach 2 is the method proposed in this study. Because the deviation cost of Approach 1 is always zero, only steps 2.1 and 2.2.2 in Table 6 are performed. In the three scenarios, the application of our proposed method reduced the station dwell time of loaded railcars by 3.69%, 3.78%, and 5.91%, while the fulfillment rate of the loading plan improved by 3.61%, 5.71%, and 6.77%, respectively. The results indicate that, across all scenarios, the proposed method consistently improves both transportation efficiency and loading fulfillment rate, confirming that collaborative optimization is effective in enhancing service quality.

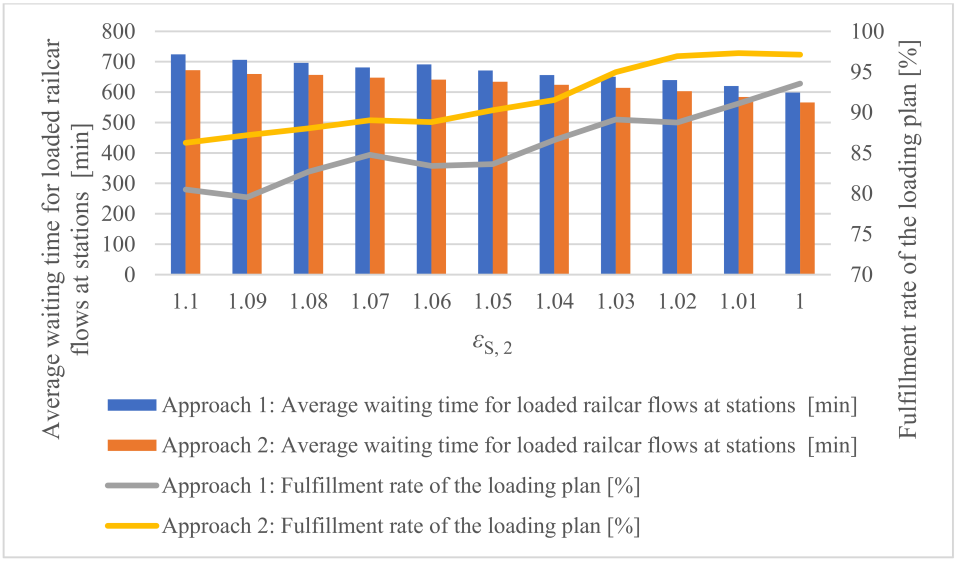


(**a**)

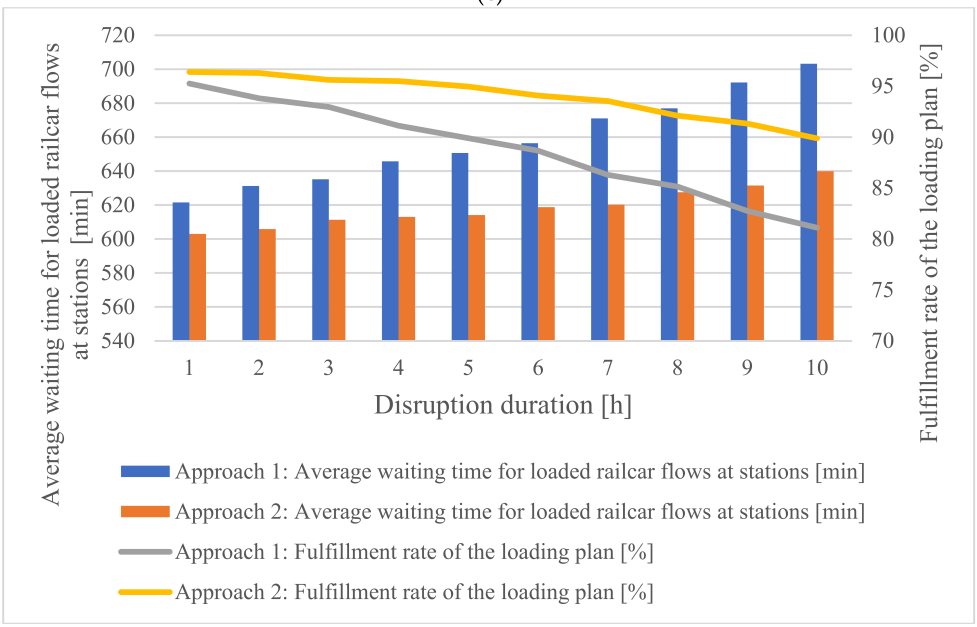


(**b**)

Figure 17. *Cont.*



(**c**)



(**d**)

Figure 17. (**a**) Comparison with the baseline (Scenario 1). (**b**) Comparison with the baseline (Scenario 2). (**c**) Comparison with the baseline (Scenario 3). (**d**) Comparison with the baseline under varying disruption durations (Scenario 3).

To further investigate the impact of disruption duration on the experimental results, Scenario 3 is taken as an example with $\varepsilon_{S,2}$ = 1.03, and the results are presented in Figure 17d. It can be observed that as the disruption duration increases, the optimization effect of the proposed method becomes more pronounced.

(2) Computational efficiency

The CPU times recorded in Appendix D indicate that, in all scenarios, except for the case where $\varepsilon_{S,2}$ is very small (e.g., 1 or 1.01, which is extreme according to the above analysis and is not recommended), a feasible solution with a gap of less than 0.1% can be found within the allotted time for each step. However, due to the scarcity of relevant literature, there is no benchmark for comparison. Although Qu and He [7] addressed a similar problem, the space–time network they constructed contained only 584 arcs. By contrast, the space–time network in this paper is much larger, comprising over 20,000 arcs, which

makes direct comparisons impractical. Further algorithm testing on space–time networks of varying sizes is being considered to assess the method's performance thoroughly. Ten new cases are generated, as detailed in 2–11 in Table 10.

Table 10. Problem instances.

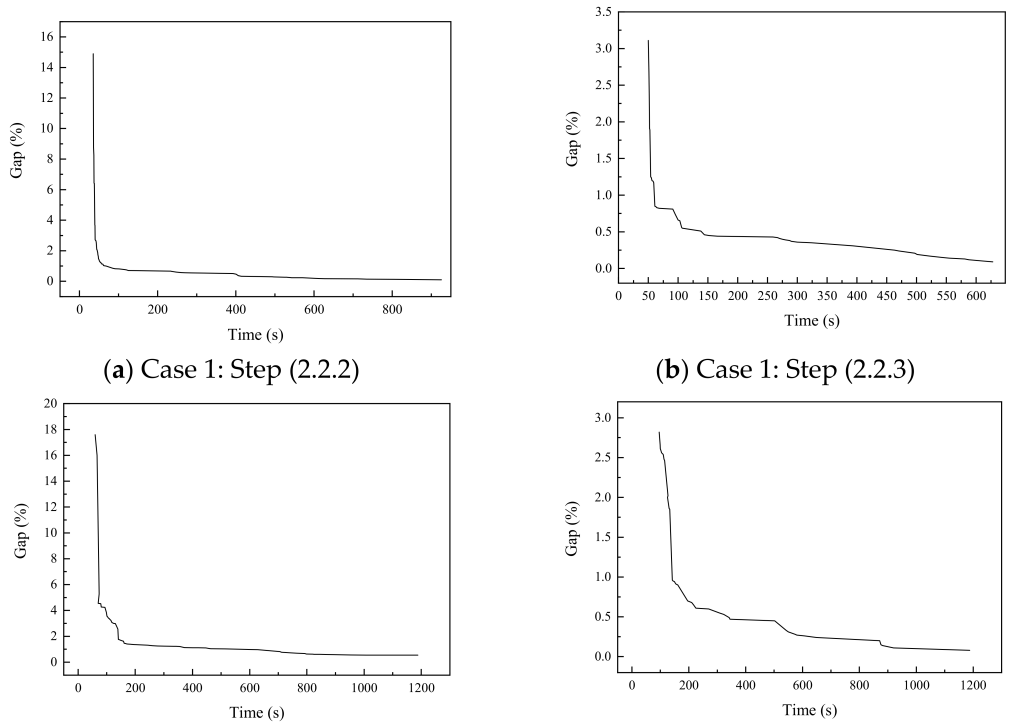
Index	$\|L_V\|$	$\|L\|$	Number of Variables	Number of Constraints
1	759	25,911	10,213,942	4,384,793
2	776	26,845	10,582,113	4,529,002
3	806	28,207	11,119,031	4,747,730
4	830	29,463	11,614,113	4,954,156
5	854	30,920	12,188,429	5,224,307
6	876	31,810	12,539,255	5,411,789
7	905	33,411	13,170,320	5,682,049
8	924	34,499	13,599,169	5,887,216
9	956	36,498	14,387,138	6,227,469
10	977	37,113	14,629,616	6,298,955
11	1010	39,022	15,382,075	6,628,550

Based on the previous analysis, it was observed that when $\varepsilon_{S,1}(\varepsilon_{S,2})$ is 1.03, each optimization objective sees a good trade-off. We use this value as an example to conduct the experiments for each case. According to the results presented in Table 11, it is evident that highly satisfactory feasible solutions are consistently achieved during the original plan generation (step 1) across all cases. The algorithm's computational efficiency is well within acceptable bounds, particularly considering the relatively ample decision time allocated at this stage. During the plan adjustment stage (step 2), both steps (2.1) and (2.2.1) are resolved with notable expediency. Remarkably, even in Case 8, characterized by its substantial scale, the two steps can be completed in less than 3 min, ensuring a solution gap of less than 0.1%.

Table 11. Performance of the Pareto search framework (Scenario 3, $\varepsilon_{S,2}$, $\varepsilon_{S,2} = 1.03$, $q^{\max} = 2$).

Index	CPU Time [s] (Gap < 0.1%)						CPU Time [s] (Gap < 1%)	
	Step (1.1)	Step (1.2)	Step (2.1)	Step (2.2.1)	Step (2.2.2)	Step (2.2.3)	Step (2.2.2)	Step (2.2.3)
1	1200 (0.42%)	1200 (1.20%)	66	47	926	628	50	61
2	1200 (0.26%)	1200 (1.29%)	76	42	806	742	84	58
3	1200 (0.29%)	1200 (1.12%)	54	48	936	978	89	65
4	1200 (0.33%)	1200 (1.71%)	58	49	1200 (0.17%)	847	140	61
5	1200 (0.38%)	1200 (2.06%)	145	71	1200 (0.17%)	893	224	104
6	1200 (0.42%)	1200 (1.15%)	98	56	1200 (0.24%)	1200 (0.12%)	138	130
7	1200 (0.34%)	1200 (2.72%)	100	66	1200 (0.30%)	1200 (0.17%)	326	170
8	1200 (0.36%)	1200 (3.26%)	73	65	1200 (0.29%)	1200 (0.15%)	537	196
9	1200 (0.41%)	1200 (3.29%)	143	72	1200 (0.37%)	1200 (0.12%)	475	185
10	1200 (0.39%)	1200 (3.97%)	96	73	1200 (0.60%)	1200 (0.40%)	772	357
11	1200 (0.44%)	1200 (3.10%)	166	90	1200 (0.54%)	1188	604	142

Although steps (2.2.2) and (2.2.3) necessitate a relatively longer duration, Figure 18 demonstrates a rapid decrease in the gap. For instance, in Case 1, the solution was achieved within 2 min to reach a gap of less than 1%. By marginally increasing the termination gap of the solver, a high-quality, feasible solution can be obtained in a shorter duration.



(**a**) Case 1: Step (2.2.2) (**b**) Case 1: Step (2.2.3)

(**c**) Case 11: Step (2.2.2) (**d**) Case 11: Step (2.2.3)

Figure 18. Solution gap over time.

5. Conclusions

The real-time rescheduling of freight trains is crucial for railroad operators to manage unexpected events effectively. However, current practice still relies heavily on manual adjustments by dispatchers, and existing studies have never jointly solved freight train rescheduling and railcar flow rerouting, despite their tight coupling in real-world operations. Neglecting this interdependence may compromise solution feasibility and service quality. To address this gap, this paper establishes a two-layer space–time network model and develops an adapted Pareto-based search framework to achieve effective trade-offs among multiple optimization objectives.

The experimental results directly support the following findings. First, jointly optimizing train rescheduling and railcar flow rerouting effectively improves service quality, reducing the station dwell time of loaded railcars by more than 3% across all three scenarios, and the improvement becomes more pronounced as the scale of the disruption increases. Second, transportation efficiency, operational cost, and plan stability cannot be simultaneously optimized, yet their interrelationships exhibit highly consistent patterns across different disruption scenarios. Third, in scenarios involving segment blockage, the introduction of candidate physical routes effectively enhances service quality, and the level of improvement becomes more noticeable as the number of candidate routes increases. Incorporating alternative routes yields a 2.3% reduction in shipment travel time cost.

From a managerial perspective, the results suggest that during the plan adjustment process, moderate changes to the timetable structure are highly cost-effective, while excessive adjustments offer little additional benefit and should be avoided. In addition, dispatchers may allow a modest reduction in transportation efficiency to control operational costs and maintain plan stability.

Several limitations should be acknowledged. First, to reduce problem complexity, the current model does not consider adjusting the position of train paths in the basic timetable during rescheduling. While this simplification avoids interfering with passenger

train operations, it inevitably limits the level of refinement achievable in plan adjustments. Second, the computational experiments indicate that under extremely large-scale networks, the current algorithm may face efficiency challenges, particularly when solving to a tight optimality gap within limited time.

Future work will extend the current framework in three directions. The first direction is to integrate freight train rescheduling with passenger train adjustments to ensure the more efficient utilization of space–time resources in mixed-traffic railways. The second direction is to incorporate differentiated time-sensitivity requirements for various commodity types by adding delivery deadlines into the model constraints. The third direction is to develop more efficient solution algorithms, including decomposition-based heuristics and machine learning-assisted pruning, to handle larger-scale instances within tighter time windows.

Funding: This research was funded by the Research Project of China Academy of Railway Sciences Corporation Limited, grant number 2025YJ128, and the Science and Technology Research and Development Program of China State Railway Group Company Limited, grant number K2026X012.

Data Availability Statement: The data that support the findings of this study are available from the corresponding author.

Conflicts of Interest: Author Bowen Ma was employed by the company Transportation and Economics Research Institute, China Academy of Railway Sciences. The author declares that the research was conducted in the absence of any commercial or financial relationships that could be construed as a potential conflict of interest.

Appendix A

Table A1. Notations used in the model formulation.

Notations	Description
Index	
m, n	Index of station
i, j	Index of physical node
t, s	Index of time
$(i,t), (j,s)$	Index of node in the space–time graph
(i,j,t,s)	Index of arc from (i,t) to (j,s)
f	Index of loaded railcar flow
$o(f)$	Index of f's origin in the space–time graph
$d(f)$	Index of f's destination in the space–time graph
$i_n^{\text{arr}}, i_n^{\text{dep}}, i_n^{\text{load}}, i_n^{\text{unload}}$	Index of ARRIVAL node, DEPARTURE node, LOADING node, UNLOADING node of the station n
Sets	
F	Set of loaded railcar flows, $f \in F$
F'	Set of railcar flows that are planned to be loaded, $F' \subseteq F$
N	Set of stations, $m, n \in N$
N_{e}	Set of boundary stations, $N_{\text{e}} \subseteq N$
N_f	Set of stations on the physical route of f, $N_f \subseteq N$

Table A1. *Cont.*

Notations	Description
V	Set of nodes in the complete space–time graph, $(i,t),(j,s) \in V$
L	Set of arcs in the complete space–time graph, $(i,j,t,s) \in L$
V^*	Set of nodes in the rescheduling space–time graph, $(i,t),(j,s) \in V^*$
L^*	Set of arcs in the rescheduling space–time graph, $(i,j,t,s) \in L^*$
L^{empty}	Set of arcs assigned with empty railcars according to the initial condition, $L^{\text{empty}} \subseteq L$
L_{train}	Set of service-layer arcs, $L_{\text{train}} \subseteq L$
$L_f^{\text{V,forbidden}}$	Set of drive arcs cannot used by f
$L_{\text{V},n}$	Set of drive arcs passing the boundary station $n \in N_{\text{e}}$, $L_{\text{V},n} \subseteq L$
$S(L)$	Set of nodes constituted by the start points of the arcs in L, $S(L) \subseteq V$
$E(L)$	Set of nodes constituted by the end points of the arcs in L, $E(L) \subseteq V$
$D(F)$	Set of f's destinations in the space–time graph, $D(F) \subseteq V$
Parameters	
c_{train}	Unit fixed cost of selecting a train path in the basic train timetable
$c_{i,j,t,s}^{f}$	Unit cost for f using the arc (i,j,t,s)
$c_{i,j,t,s}^{\text{empty}}$	Unit cost for empty railcars using the arc (i,j,t,s)
$c_{\text{punish}}^{\text{empty}}$	Unit penalty cost for not delivering empty railcars to other railroad companies through the boundary station $n \in N_{\text{e}}$
q_f	Volume of f
$q_{i,j,t,s}^{\max}$	Capacity of the arc (i,j,t,s)
$q_{i,j,t,s}^{\text{empty}}$	Empty railcar flow volume on the arc $(i,j,t,s) \in L^{\text{empty}}$ according to the initial condition
q_n^{empty}	Number of empty railcars that are planned to be delivered to other railroad companies through the boundary station $n \in N_{\text{e}}$
$\overline{x}_{i,j,t,s}^{f}$	Proportion of f distributed to the arc $(i,j,t,s) \in L$ according to the original plan
$\overline{y}_{i,j,t,s}$	Given binary value, $\overline{y}_{i,j,t,s} = 1$ if the arc $(i,j,t,s) \in L_{\text{train}}$ is used according to the original plan
$\overline{z}_{i,j,t,s}$	Number of empty railcars that are distributed to the arc $(i,j,t,s) \in L$ according to the original plan
$\overline{w}_{i,j,t,s}$	Given binary value, $\overline{w}_{i,j,t,s} = 1$ if the train using the arc $(i,j,t,s) \in L_{\text{V}}$ is disassembled after arriving at the station according to the original plan

Table A1. *Cont.*

Notations	Description
$\overline{v}_{i,j,t,s}$	Given binary value, $\overline{v}_{i,j,t,s} = 1$ if the train using the arc $(i,j,t,s) \in L_{\mathrm{V}}$ is assembled before departing from the station according to the original plan
T_{start}	Starting time of the planning horizon
T_{end}	Ending time of the planning horizon
$T_{\mathrm{reschedule}}$	Time point for reschedule decisions
$T_{\mathrm{travel}}^{f,n}$	Total running time of f being delivered from the origin station to the station $n \in N_f$
$T_{n,1}^{\mathrm{transit}}$	Average time railcars transit with resorting at the station n
$T_{n,2}^{\mathrm{transit}}$	Average time railcars transits without resorting at the station n
$T_n^{\mathrm{disassemble}}$	Sum of a train's arrival technical operation time and disassembling operation time at the station n
T_n^{assemble}	Sum of a train's assembling operation time and departure technical operation time at the station n
T_n^{takeout}	Average time railcars are picked from loading yard to shunting yard at the station n
T_n^{placein}	Average time railcars are delivered from shunting yard to loading yard at the station n
T_n^{load}	Average time empty railcars are loaded at the station n
T_n^{unload}	Average time loaded railcars are unloaded at the station n
Decision variables	
$x_{i,j,t,s}^{f}$	Proportion of f distributed to the arc $(i,j,t,s) \in L$
$y_{i,j,t,s}$	Binary variable, $y_{i,j,t,s} = 1$ if the arc $(i,j,t,s) \in L_{\mathrm{train}}$ is used
$z_{i,j,t,s}$	Number of empty railcars that are distributed to the arc $(i,j,t,s) \in L$
$w_{i,j,t,s}$	Binary variable, $w_{i,j,t,s} = 1$ if the train using the arc $(i,j,t,s) \in L_{\mathrm{V}}$ is disassembled after arriving at the station
$v_{i,j,t,s}$	Binary variable, $v_{i,j,t,s}$ if the train using the arc $(i,j,t,s) \in L_{\mathrm{V}}$ is assembled before departing from the station

Appendix B

Table A2. Definition of $o(f)$.

Index	Status of the Loaded Railcar Flow at the Beginning of the Planning Horizon	$o(f)$	
		Physical Node	**Time Node**
1	Arriving or already arrived at station $n \in N_f$	i_n^{arr}	The time that f arrives at station $n \in N_f$
2	Loading or already loaded at the loading station n	i_n^{dep}	The earliest time that f could depart from station n
3	Wait to be loaded at the loading station n	i_n^{load}	T_{start}

Table A3. Definition of $d(f)$.

Index	Possible Status of the Loaded Railcar Flow at the End of the Planning Horizon	$d(f)$	
		Physical Node	**Time Node**
1	Arriving or already arrived at station $n \in N_f$	i_n^{arr}	T_{end}
2	Staying at the loading station n after loaded	i_n^{dep}	
3	Already unloaded at the unloading station n	i_n^{unload}	
4	Not loaded	i_n^{load}	

Appendix C

Algorithm A1 The algorithm for exploring Pareto frontier based on ε constraints

Step 0: Initialization

The set of Pareto-optimal solutions of the rescheduling problem $P = \varnothing$.

Step 1: Obtain the original train operation plan

Step 1.1: Compute the worst value of Z_S ($Z_S^{U,1}$)

Obtain $Z_S^{U,1}$ by solving the model with Z_S as the objective function, constraints consist of (4)–(21), (24)–(28).

Step 1.2: Determine the upper bound of Z_S, then solve the model with added ε constraints

For $\varepsilon_{S,1}$

Solve the model with Z_O as the objective function, constraints consist of (4)–(21), (24)–(28), (36).

End For

Step 1.3: Select a non-dominated solution from the solutions obtained in step 1.2 as the input of the rescheduling problem

Step 2: Explore the three-dimensional Pareto frontier of the rescheduling problem

Step 2.1: Compute the optimal value of Z_S ($Z_S^{U,2}$)

Solve the model with Z_S as the objective function, constraints consist of (4)–(28), (30)–(33).

Step 2.2: Solve the model with added ε constraints

For $\varepsilon_{S,2}$

Step 2.2.1: Compute an optimal value of Z_D (Z_D^U)

Obtain Z_D^U by solving the model with Z_D as the objective function, constraints consist of (4)–(28), (30)–(33), (37).

Step 2.2.2: Compute an inferior value of Z_D (Z_D^{SN})

Solve the model with Z_O as the objective function, constraints consist of (4)–(28), (30)–(33), (37). The optimal solution is x_O^U. Obtain Z_D^{SN} by substituting x_O^U into Z_D.

Step 2.2.3: Determine the upper bound of Z_S and Z_D, then solve the model with added ε constraints

For ε_D

Solve the model with Z_O as the objective function, constraints consist of (4)–(28), (30)–(33), (37), (38).

End For

End For

Step 3: Generate the Pareto frontier

Add the solutions obtained in step 2 to P and eliminate the non-Pareto-optimal solutions in P.

Appendix D. Pareto Solutions

Table A4. Pareto solutions for Scenario 1.

$\varepsilon_{S,2}$	ε_D	Z_S	Z_O	Z_D	CPU Time [s]	Related Indicators After Rescheduling						Deviation from the Original Plan			
						TO	PS	WT^1 [Min]	WT^2 [Min]	WT^3 [Min]	FL [%]	PNS	PC	AA	HA
1.1	129 *	340,908	1,794,788	129	261	277	340	289.76	861.15	687.39	90.39	11	112	2	4
1.1	109	340,908	1,797,373	108	194	278	341	293.28	855.48	684.51	90.89	3	103	0	2
1.1	90	340,907	1,856,329	90	33	290	353	299.53	847.05	680.55	90.59	0	88	0	2
1.1	70	340,908	1,957,313	70	34	304	373	291.13	844.83	676.45	87.82	0	68	0	2
1.1	31	340,908	2,151,329	31	31	345	412	293.35	831.68	667.97	83.92	0	29	0	2
1.09	118 *	337,809	1,832,516	118	398	281	348	278.23	851.54	677.20	90.67	10	103	2	3
1.09	100	337,808	1,836,545	100	232	283	349	281.11	848.01	675.61	90.89	3	95	0	2
1.09	82	337,809	1,896,329	82	42	295	361	279.31	844.76	672.80	90.27	0	80	0	2
1.09	29	337,809	2,161,329	29	33	344	414	288.40	817.15	656.36	86.07	0	27	0	2
1.08	118 *	334,710	1,874,642	118	517	286	356	269.86	842.97	668.69	90.73	13	98	3	4
1.08	100	334,710	1,875,180	99	297	286	356	270.77	842.87	668.89	90.77	5	90	1	3
1.08	82	334,710	1,896,344	82	54	291	361	272.03	837.72	665.70	90.75	0	80	0	2
1.08	47	334,616	2,071,329	47	32	319	396	275.78	815.23	651.18	89.73	0	45	0	2
1.08	29	334,710	2,161,709	29	30	347	414	282.25	801.62	643.68	88.72	0	27	0	2
1.07	12 **	331,611	2,460,262	12	40	344	431	263.77	812.79	645.83	88.38	0	10	0	2
1.07	92 *	331,610	1,920,939	92	370	293	365	262.85	832.25	659.10	91.17	7	83	0	2
1.07	78	331,611	1,929,765	78	81	292	367	258.42	836.39	660.63	91.03	1	75	0	2
1.07	65	331,589	1,981,329	65	39	300	378	263.57	827.79	656.21	90.79	0	63	0	2
1.07	52	331,610	2,046,329	52	32	314	391	268.66	816.13	649.65	90.39	0	50	0	2
1.06	12 **	328,496	2,480,337	12	38	359	431	277.46	782.86	629.17	92.16	0	10	0	2
1.06	91 *	328,512	1,976,425	91	387	296	375	253.50	822.66	649.58	91.24	11	77	1	2
1.06	77	328,512	1,976,979	77	299	299	376	257.56	817.56	647.26	91.21	5	70	0	2
1.06	64	328,511	1,991,256	64	68	301	379	256.86	817.10	646.73	91.07	0	62	0	2
1.06	51	328,511	2,051,329	51	39	312	392	252.90	815.36	644.32	90.73	0	49	0	2
1.06	38	328,512	2,116,329	38	32	329	405	263.13	797.18	634.77	90.17	0	36	0	2
1.06	25	328,512	2,181,329	25	31	336	418	257.87	802.70	637.02	88.55	0	23	0	2
1.05	68	325,412	2,039,687	68	268	306	387	251.50	803.64	635.73	91.63	6	60	0	2
1.05	57	325,412	2,047,581	57	78	309	390	253.84	801.66	635.06	91.76	2	53	0	2
1.05	46	325,413	2,078,412	46	47	314	397	249.37	801.57	633.64	91.43	0	44	0	2

Table A4. *Cont.*

$\varepsilon_{S,2}$	ε_D	Z_S	Z_O	Z_D	CPU Time [s]	Related Indicators After Rescheduling						Deviation from the Original Plan			
						TO	PS	WT^1 [Min]	WT^2 [Min]	WT^3 [Min]	FL [%]	PNS	PC	AA	HA
1.05	34	325,413	2,136,329	34	34	325	409	252.90	790.87	627.27	91.30	0	32	0	2
1.05	23	325,412	2,192,528	23	32	338	420	258.60	784.09	624.29	90.71	0	21	0	2
1.04	12 **	322,282	2,482,179	12	38	350	431	254.60	775.99	617.44	94.51	0	10	0	2
1.04	66	322,313	2,116,661	64	346	317	401	247.07	789.24	624.37	92.52	10	50	1	3
1.04	55	322,313	2,117,006	54	263	318	401	244.64	790.88	624.76	92.41	6	46	0	2
1.04	44	322,313	2,125,365	44	65	319	403	246.56	789.07	624.09	92.60	2	40	0	2
1.04	33	322,313	2,148,653	33	37	323	410	251.26	780.31	619.43	91.75	0	31	0	2
1.04	22	322,313	2,198,499	22	36	328	421	248.60	780.92	619.04	91.82	0	20	0	2
1.03	12 **	319,210	2,487,373	12	41	341	431	249.72	767.34	609.93	96.62	0	10	0	2
1.03	47	319,214	2,217,015	44	594	331	419	246.46	773.43	613.18	96.35	9	31	1	3
1.03	40	319,214	2,217,392	40	281	332	419	244.38	775.14	613.73	96.37	7	29	1	3
1.03	33	319,214	2,219,555	33	118	331	420	245.74	772.83	612.54	95.46	5	26	0	2
1.03	26	319,214	2,227,463	26	152	331	421	248.16	773.29	613.60	96.48	2	22	0	2
1.03	19	319,214	2,240,583	19	79	337	426	248.01	769.37	610.83	96.41	1	16	0	2
1.02	26 **	316,112	2,564,651	26	75	352	445	245.45	751.75	597.78	98.24	14	10	0	2
1.02	55	316,115	2,330,530	55	952	344	441	242.60	755.50	599.52	97.76	20	20	7	8
1.02	49	316,115	2,331,468	49	976	345	441	242.60	755.97	599.85	98.15	18	18	6	7
1.02	43	316,115	2,332,451	42	804	346	441	243.72	753.00	598.12	97.78	16	16	4	6
1.02	37	316,115	2,335,758	37	437	349	442	242.14	754.59	598.75	98.08	16	15	2	4
1.02	31	316,115	2,342,107	31	304	347	442	244.85	751.77	597.62	98.20	13	12	2	4
1.01	72 **	313,008	2,715,242	72	73	373	475	241.52	726.43	578.97	98.40	44	10	8	10
1.01	110 *	313,015	2,475,194	110	1200 (0.27%)	361	469	241.34	730.37	581.65	98.16	50	22	19	19
1.01	103	313,016	2,475,353	103	1200 (0.33%)	360	469	241.37	730.72	581.91	98.16	47	19	18	19
1.01	97	313,016	2,475,715	96	1200 (0.31%)	362	469	241.56	729.67	581.24	98.20	45	17	16	18
1.01	91	313,015	2,476,279	90	1200 (0.19%)	361	469	241.33	730.32	581.62	98.20	42	14	16	18
1.01	84	313,016	2,482,275	83	1200 (0.22%)	363	470	241.34	729.76	581.23	98.41	41	12	14	16
1.01	78	313,016	2,491,712	78	1200 (0.34%)	367	471	241.34	728.14	580.10	98.42	42	12	11	13
1	227 **	309,917	3,099,819	227	1200 (12.2%)	413	551	241.19	699.22	559.93	98.12	120	10	48	49
1	245 *	309,917	2,884,150	245	1200 (2.67%)	404	541	241.93	699.17	560.13	98.12	121	21	52	51

Deviation from the original plan: number of train paths newly selected (PNS), number of train paths canceled (PC), number of assembling tasks added at unplanned time points (AA), number of humping tasks added at unplanned time points (HA). The second column of numbers with corner notation ** and * indicates that the solution was obtained through steps (2.2.1) and (2.2.2), respectively, while the absence of a corner notation indicates that the solution was obtained through step (2.2.3).

Table A5. Pareto solutions for Scenario 2.

$\varepsilon_{S,2}$	ε_D	Z_S	Z_O	Z_D	CPU Time [s]	Related Indicators After Rescheduling						Deviation from the Original Plan			
						TO	PS	WT^1 [Min]	WT^2 [Min]	WT^3 [Min]	FL [%]	PNS	PC	AA	HA
1.1	84 *	355,060	1,878,130	84	40	283	355	301.30	864.53	693.25	92.17	4	80	0	0
1.1	70	355,055	1,907,412	70	31	289	361	296.73	868.67	694.74	90.14	0	70	0	0
1.1	56	355,060	1,977,412	56	28	302	375	299.67	859.40	689.19	84.65	0	56	0	0
1.1	42	355,060	2,047,412	42	32	318	389	308.27	847.21	683.32	85.96	0	42	0	0
1.09	75 *	351,830	1,911,599	75	59	289	362	297.31	849.53	681.60	92.72	3	72	0	0
1.09	62	351,830	1,947,412	62	36	294	369	278.89	863.65	685.83	91.00	0	62	0	0
1.09	50	351,830	2,007,412	50	32	308	381	294.01	844.86	677.34	85.93	0	50	0	0
1.09	37	351,830	2,072,412	37	28	319	394	291.49	841.90	674.52	80.03	0	37	0	0
1.09	25	351,832	2,132,412	25	28	332	406	290.71	833.27	668.28	83.22	0	25	0	0
1.09	12	351,832	2,197,412	12	28	336	419	298.45	833.13	670.53	80.04	0	12	0	0
1.08	69 *	348,605	1,945,947	69	74	292	368	282.79	846.53	675.10	92.71	3	66	0	0
1.08	57	348,605	1,972,412	57	31	298	374	282.58	846.25	674.84	91.36	0	57	0	0
1.08	46	348,604	2,027,412	46	29	304	385	278.57	849.30	675.74	88.77	0	46	0	0
1.08	34	348,605	2,087,412	34	28	319	397	281.53	839.25	669.65	88.80	0	34	0	0
1.08	23	348,588	2,142,412	23	28	329	408	289.97	822.69	660.69	84.51	0	23	0	0
1.07	62 *	345,375	1,982,367	62	57	296	376	271.91	838.26	666.03	92.70	3	58	0	1
1.07	51	345,377	2,002,412	51	32	297	380	263.32	847.45	669.82	91.74	0	51	0	0
1.07	41	345,234	2,052,412	41	28	312	390	274.07	832.57	662.73	88.72	0	41	0	0
1.07	31	345,377	2,102,412	31	27	323	400	274.21	822.83	655.99	86.53	0	31	0	0
1.07	20	345,377	2,157,412	20	27	331	411	284.20	812.46	651.82	85.81	0	20	0	0
1.07	10	345,376	2,207,412	10	27	334	421	280.88	816.27	653.46	83.00	0	10	0	0
1.06	0 **	342,149	2,406,513	0	34	348	431	279.83	803.27	644.09	89.27	0	0	0	0
1.06	53 *	342,149	2,022,729	53	59	299	384	258.73	833.05	658.40	92.70	3	50	0	0
1.06	44	342,146	2,037,412	44	32	304	387	258.50	832.13	657.69	92.39	0	44	0	0
1.06	35	342,149	2,082,412	35	30	310	396	254.41	833.65	657.50	90.75	0	35	0	0
1.06	26	342,149	2,127,412	26	28	318	405	263.88	823.10	653.05	90.32	0	26	0	0
1.06	17	342,149	2,172,412	17	28	328	414	258.07	824.47	652.23	86.22	0	17	0	0
1.06	8	342,149	2,217,412	8	27	338	423	258.08	818.82	648.30	88.73	0	8	0	0
1.05	0 **	338,921	2,418,213	0	34	342	431	263.09	801.05	637.45	90.16	0	0	0	0
1.05	43 *	338,920	2,069,930	43	62	303	392	250.62	823.85	649.53	92.71	2	41	0	0
1.05	35	338,921	2,082,492	35	35	312	396	255.21	816.25	645.64	92.79	0	35	0	0

Table A5. *Cont.*

$\varepsilon_{S,2}$	ε_D	Z_S	Z_O	Z_D	CPU Time [s]	Related Indicators After Rescheduling						Deviation from the Original Plan			
						TO	PS	WT^1 [Min]	WT^2 [Min]	WT^3 [Min]	FL [%]	PNS	PC	AA	HA
1.05	28	338,894	2,117,412	28	29	317	403	249.15	819.52	646.07	91.62	0	28	0	0
1.05	21	338,914	2,152,412	21	29	318	410	251.22	819.56	646.73	90.44	0	21	0	0
1.05	14	338,787	2,187,412	14	28	329	417	251.86	808.74	639.39	89.10	0	14	0	0
1.05	7	338,920	2,222,412	7	27	336	424	254.92	805.63	638.16	88.68	0	7	0	0
1.04	0 **	335,693	2,423,742	0	34	335	431	249.53	798.99	631.90	90.40	0	0	0	0
1.04	35 *	335,693	2,129,876	35	124	315	404	246.07	808.37	637.37	92.88	4	31	0	0
1.04	29	335,693	2,130,092	29	48	314	404	244.18	808.52	636.91	92.71	1	28	0	0
1.04	23	335,693	2,143,063	23	30	318	408	243.60	807.92	636.31	92.55	0	23	0	0
1.04	17	335,693	2,172,588	17	28	326	414	246.49	802.55	633.45	92.25	0	17	0	0
1.04	11	335,692	2,202,412	11	29	327	420	247.02	802.55	633.61	91.54	0	11	0	0
1.04	5	335,693	2,232,412	5	28	331	426	247.65	800.96	632.69	90.73	0	5	0	0
1.03	0 **	332,465	2,428,878	0	34	336	431	243.07	787.19	621.72	92.61	0	0	0	0
1.03	20	332,465	2,210,384	19	171	325	419	240.78	792.86	624.97	93.64	3	15	1	0
1.03	15	332,465	2,210,591	14	65	325	419	240.78	792.67	624.84	93.33	1	13	0	0
1.03	10	332,464	2,217,438	10	31	326	421	240.46	791.22	623.73	93.04	0	10	0	0
1.03	5	332,466	2,234,795	5	29	330	426	242.07	786.79	621.14	93.04	0	5	0	0
1.02	8 *	329,235	2,478,768	8	42	342	439	239.92	772.97	610.87	96.42	8	0	0	0
1.02	21	329,237	2,320,561	21	199	341	440	238.57	772.74	610.30	95.56	12	3	3	3
1.02	17	329,237	2,322,939	17	697	343	440	240.30	771.71	610.11	96.06	12	3	1	1
1.02	12	329,238	2,324,659	12	112	341	439	240.30	772.42	610.60	96.34	9	1	1	1
1.01	50 **	326,010	2,641,130	50	91	369	471	236.25	747.71	592.18	96.81	40	0	5	5
1.01	76 *	326,010	2,467,530	76	1200 (0.38%)	357	468	236.95	750.37	594.24	96.58	41	4	15	16
1.01	67	326,010	2,468,773	67	1200 (0.45%)	357	468	236.94	750.41	594.27	96.58	38	1	14	14
1.01	63	326,009	2,471,279	63	1200 (0.41%)	361	469	236.69	749.18	593.33	96.79	39	1	12	11
1.01	58	326,008	2,476,372	58	1200 (0.23%)	362	469	236.44	748.74	592.95	96.65	38	0	10	10
1.01	54	326,010	2,485,501	54	1200 (0.27%)	364	469	236.62	747.41	592.08	96.65	38	0	8	8
1	186 **	322,782	2,991,787	186	1200 (2.84%)	406	541	236.42	720.59	573.35	96.92	110	0	38	38
1	199 *	322,781	2,847,492	199	1200 (0.98%)	397	535	236.42	720.59	573.35	96.92	110	0	38	38
1	196	322,782	2,847,492	193	1200 (0.95%)	398	535	237.48	719.89	573.19	96.92	108	4	44	43

Table A6. Pareto solutions for Scenario 3 (AP-NCR).

$\varepsilon_{S,2}$	ε_D	Z_S	Z_O	Z_D	CPU Time [s]	Related Indicators After Rescheduling						Deviation from the Original Plan			
						TO	PS	WT^1 [Min]	WT^2 [Min]	WT^3 [Min]	FL [%]	PNS	PC	AA	HA
1.1	20 *	347,934	2,439,495	20	40	357	423	322.98	821.14	669.65	86.96	0	17	0	3
1.1	135 **	347,934	1,765,510	135	245	268	335	295.53	870.31	695.51	89.43	11	116	3	5
1.1	115	347,934	1,769,237	114	151	270	335	301.40	865.02	693.63	89.41	2	107	1	4
1.1	96	347,932	1,826,097	96	42	283	347	288.34	871.95	694.48	87.31	0	93	0	3
1.1	77	347,932	1,921,121	77	37	303	366	312.50	838.62	678.62	88.74	0	74	0	3
1.1	58	347,933	2,016,097	58	35	320	385	312.01	825.64	669.45	87.54	0	55	0	3
1.1	39	347,933	2,111,097	39	35	339	404	312.38	829.48	672.23	86.25	0	36	0	3
1.09	130 *	344,770	1,805,730	130	609	275	343	287.88	858.47	684.95	89.43	11	108	4	7
1.09	111	344,770	1,807,057	111	123	275	343	285.44	860.91	685.91	89.43	4	101	2	4
1.09	93	344,770	1,841,097	93	49	276	350	280.63	867.09	688.74	89.39	0	90	0	3
1.09	75	344,771	1,931,097	75	39	300	368	300.93	833.11	671.27	89.85	0	72	0	3
1.09	56	344,764	2,027,025	56	39	323	387	295.20	825.11	663.96	88.07	0	53	0	3
1.09	38	344,771	2,116,097	38	34	338	405	309.78	812.50	659.63	87.18	0	35	0	3
1.08	20 **	341,608	2,440,856	20	45	353	423	310.44	805.29	654.80	87.48	0	17	0	3
1.08	126 *	341,608	1,847,295	126	465	279	351	277.12	850.95	676.45	89.75	13	102	4	7
1.08	108	341,608	1,848,340	107	295	279	351	277.48	849.56	675.59	89.84	6	95	2	4
1.08	90	341,606	1,862,549	90	122	281	353	283.18	845.20	674.29	90.20	0	87	0	3
1.08	73	341,608	1,941,097	73	39	301	370	297.36	823.28	663.34	89.53	0	70	0	3
1.08	55	341,608	2,031,114	55	35	314	388	293.53	819.00	659.21	87.58	0	52	0	3
1.08	37	341,603	2,121,097	37	48	338	406	286.94	817.82	656.38	88.03	0	34	0	3
1.07	20 **	338,445	2,441,624	20	48	353	423	280.66	801.89	643.38	92.72	0	17	0	3
1.07	111 *	338,445	1,897,112	111	986	285	361	269.79	839.13	665.99	90.15	10	89	4	8
1.07	95	338,445	1,898,806	95	408	287	361	275.68	833.76	664.05	90.17	5	84	2	4
1.07	80	338,445	1,912,940	80	158	287	363	273.44	836.26	665.10	90.40	0	77	0	3
1.07	65	338,445	1,981,594	65	40	304	378	281.35	820.77	656.74	90.40	0	62	0	3
1.07	50	338,445	2,056,097	50	35	323	393	288.32	810.17	651.48	89.14	0	47	0	3
1.07	35	338,445	2,131,337	35	34	327	408	287.43	805.08	647.66	89.02	0	32	0	3
1.06	97 *	335,282	1,953,064	97	1012	290	371	266.58	823.99	654.49	90.13	9	78	4	6
1.06	84	335,281	1,955,047	84	435	293	372	266.84	821.84	653.06	90.23	5	73	2	4
1.06	71	335,281	1,966,143	71	66	296	374	264.66	822.98	653.20	90.35	1	67	0	3
1.06	58	335,282	2,016,653	58	60	304	385	265.54	817.81	649.86	90.12	0	55	0	3

Table A6. *Cont.*

$\varepsilon_{S,2}$	ε_D	Z_S	Z_O	Z_D	CPU Time [s]	Related Indicators After Rescheduling						Deviation from the Original Plan			
						TO	PS	WT^1 [Min]	WT^2 [Min]	WT^3 [Min]	FL [%]	PNS	PC	AA	HA
1.06	45	335,275	2,081,097	45	39	309	398	270.12	811.31	646.74	89.95	0	42	0	3
1.06	32	335,282	2,146,097	32	34	331	411	267.38	804.19	640.95	88.80	0	29	0	3
1.05	20 **	332,091	2,448,762	20	40	345	423	268.20	790.34	631.56	93.26	0	17	0	3
1.05	100 *	332,119	2,019,594	100	972	298	384	260.15	810.32	643.01	90.74	15	71	5	9
1.05	86	332,119	2,020,347	84	1066	300	384	259.77	808.64	641.73	90.78	10	66	3	5
1.05	73	332,119	2,020,951	73	519	301	383	258.98	810.21	642.58	90.93	5	62	2	4
1.05	60	332,119	2,032,440	60	171	304	385	257.10	809.12	641.25	91.07	1	56	0	3
1.05	46	332,119	2,077,003	46	69	310	397	262.56	800.28	636.76	90.93	0	43	0	3
1.05	33	332,118	2,141,097	33	37	323	410	262.24	796.40	633.96	90.27	0	30	0	3
1.04	20 **	328,873	2,450,189	20	39	342	423	265.48	777.79	622.00	94.93	0	17	0	3
1.04	75	328,956	2,098,676	74	919	313	398	254.66	793.19	629.43	92.03	11	53	3	7
1.04	64	328,956	2,102,286	64	735	313	399	254.32	793.61	629.61	92.04	7	48	3	6
1.04	53	328,956	2,107,785	53	442	315	400	254.00	790.78	627.54	92.49	4	44	2	3
1.04	42	328,955	2,122,917	42	108	318	403	253.47	791.29	627.74	92.30	1	38	0	3
1.04	31	328,956	2,157,143	31	50	321	412	261.95	781.98	623.84	91.53	0	28	0	3
1.03	21 **	325,793	2,457,488	21	47	334	424	254.81	772.94	615.38	95.71	1	17	0	3
1.03	78 *	325,793	2,198,228	78	926	324	417	253.94	775.35	616.79	94.03	20	43	5	10
1.03	59	325,793	2,198,824	59	840	324	417	253.86	775.17	616.64	94.03	13	36	3	7
1.03	49	325,793	2,202,206	49	628	324	417	255.68	776.17	617.89	95.04	8	31	3	7
1.03	40	325,793	2,207,325	40	486	324	419	254.50	773.53	615.70	93.76	6	27	2	5
1.03	30	325,793	2,214,814	30	235	328	420	255.47	770.75	614.05	94.96	3	23	1	3
1.02	42 **	322,628	2,568,329	42	110	352	445	253.38	750.86	599.58	97.20	22	17	0	3
1.02	81 *	322,630	2,310,476	80	1200 (0.16%)	339	438	250.53	755.58	601.99	96.39	28	30	9	13
1.02	65	322,630	2,310,718	64	934	338	438	250.70	757.34	603.27	96.50	21	23	8	12
1.02	57	322,630	2,311,397	56	692	339	438	251.89	756.21	602.84	96.50	19	21	6	10
1.02	49	322,630	2,319,026	49	481	343	439	253.61	755.60	602.95	96.94	18	19	4	8
1.01	90 **	319,466	2,715,590	90	1200 (2.86%)	373	474	248.10	728.79	582.61	97.23	51	17	9	13
1.01	131 *	319,467	2,458,540	131	1200 (0.25%)	355	467	248.26	734.65	586.74	97.12	55	28	21	27
1.01	124	319,467	2,459,280	124	1200 (0.44%)	354	467	248.83	734.09	586.52	96.87	51	24	23	26
1.01	117	319,467	2,459,489	117	1200 (0.56%)	355	467	248.31	734.43	586.60	96.96	49	22	21	25
1.01	110	319,467	2,461,167	110	1200 (0.35%)	358	467	248.00	733.50	585.86	97.11	49	22	17	22

Table A6. *Cont.*

$\varepsilon_{S,2}$	ε_D	Z_S	Z_O	Z_D	CPU Time [s]	Related Indicators After Rescheduling						Deviation from the Original Plan			
						TO	PS	WT^1 [Min]	WT^2 [Min]	WT^3 [Min]	FL [%]	PNS	PC	AA	HA
1.01	103	319,467	2,466,186	103	1200 (0.37%)	360	467	249.18	732.34	585.41	97.31	48	21	15	19
1.01	96	319,467	2,485,936	96	1200 (0.81%)	366	470	248.27	730.80	584.06	97.31	49	19	12	16
1	259 **	316,305	3,119,653	259	1200 (13.36%)	413	554	246.46	704.94	565.51	97.24	131	17	54	57
1	279 *	316,306	2,904,247	279	1200 (4.09%)	401	545	248.62	704.73	566.03	97.12	131	26	59	63

References

1. Frisch, S.; Hungerlnde, P.; Jellen, A.; Lackenbucher, M.; Primas, B.; Steininger, S. Integrated Freight Car Routing and Train Scheduling. *Cent. Eur. J. Oper. Res.* **2022**, *31*, 417–443. [CrossRef]
2. Lin, B.; Zhao, Y.; Lin, R.; Liu, C. Integrating Traffic Routing Optimization and Train Formation Plan Using Simulated Annealing Algorithm. *Appl. Math. Model.* **2021**, *93*, 811–830. [CrossRef]
3. Ahuja, R.K.; Jha, K.C.; Liu, J. Solving Real-Life Railroad Blocking Problems. *Interfaces* **2007**, *37*, 404–419. [CrossRef]
4. Assad, A.A. Modelling of Rail Networks: Toward a Routing/Makeup Model. *Transp. Res. Part B* **1980**, *14*, 101–114. [CrossRef]
5. Ma, B.; Wei, Y.; Fang, B.; Qu, C. Research on Railway Dynamic Car Flow Organization for Railway Bureau-Station Integration. *J. China Railw. Soc.* **2023**, *45*, 1–11. [CrossRef]
6. Li, S.; Lv, H.; Xu, C.; Chen, T.; Zou, C. Optimized Train Path Selection Method for Daily Freight Train Scheduling. *IEEE Access* **2020**, *8*, 40777–40790. [CrossRef]
7. Qu, Z.; He, S. A Time-Space Network Model Based on a Train Diagram for Predicting and Controlling the Traffic Congestion in a Station Caused by an Emergency. *Symmetry* **2019**, *11*, 780. [CrossRef]
8. Zhan, S.; Wong, S.C.; Shang, P.; Peng, Q.; Xie, J.; Lo, S.M. Integrated Railway Timetable Rescheduling and Dynamic Passenger Routing During a Complete Blockage. *Transp. Res. Part B Methodol.* **2021**, *143*, 86–123. [CrossRef]
9. Zhu, E.D.; Crainic, T.G.; Gendreau, M. Scheduled Service Network Design for Freight Rail Transportation. *Oper. Res.* **2014**, *62*, 383–400. [CrossRef]
10. Odijk, M.A. A Constraint Generation Algorithm for the Construction of Periodic Railway Timetables. *Transp. Res. Part B Methodol.* **1996**, *30*, 455–464. [CrossRef]
11. Liebchen, C. The First Optimized Railway Timetable in Practice. *Transp. Sci.* **2008**, *42*, 420–435. [CrossRef]
12. Caprara, A.; Fischetti, M.; Toth, P. Modeling and Solving the Train Timetabling Problem. *Oper. Res.* **2002**, *50*, 851–861. [CrossRef]
13. Pouryousef, H.; Lautala, P.; Watkins, D. Development of Hybrid Optimization of Train Schedules Model for N-Track Rail Corridors. *Transp. Res. Part C Emerg. Technol.* **2016**, *67*, 169–192. [CrossRef]
14. Mees, A.I. Railway Scheduling by Network Optimization. *Math. Comput. Model.* **1991**, *15*, 33–42. [CrossRef]
15. Caimi, G.; Chudak, F.; Fuchsberger, M.; Laumanns, M.; Zenklusen, R. A New Resource-Constrained Multicommodity Flow Model for Conflict-Free Train Routing and Scheduling. *Transp. Sci.* **2011**, *45*, 212–227. [CrossRef]
16. Jovanović, D.; Harker, P.T. Tactical Scheduling of Rail Operations: The SCAN I System. *Transp. Sci.* **1991**, *25*, 46–64. [CrossRef]
17. Kraay, D.R.; Harker, P.T. Real-Time Scheduling of Freight Railroads. *Transp. Res. Part B Methodol.* **1995**, *29*, 213–229. [CrossRef]
18. Cacchiani, V.; Caprara, A.; Toth, P. Scheduling Extra Freight Trains on Railway Networks. *Transp. Res. Part B Methodol.* **2010**, *44*, 215–231. [CrossRef]
19. Kuo, A.; Miller-Hooks, E.; Mahmassani, H.S. Freight Train Scheduling with Elastic Demand. *Transp. Res. Part E Logist. Transp. Rev.* **2010**, *46*, 1057–1070. [CrossRef]
20. Mu, S.; Dessouky, M. Scheduling Freight Trains Traveling on Complex Networks. *Transp. Res. Part B Methodol.* **2011**, *45*, 1103–1123. [CrossRef]
21. Liu, L.; Dessouky, M.M. A Decomposition Based Hybrid Heuristic Algorithm for the Joint Passenger and Freight Train Scheduling Problem. *Comput. Oper. Res.* **2017**, *87*, 165–182. [CrossRef]
22. Liu, L.; Dessouky, M. Stochastic Passenger Train Timetabling Using a Branch and Bound Approach. *Comput. Ind. Eng.* **2018**, *127*, 1223–1240. [CrossRef]
23. Albrecht, A.R.; Panton, D.M.; Lee, D.H. Rescheduling Rail Networks with Maintenance Disruptions Using Problem Space Search. *Comput. Oper. Res.* **2013**, *40*, 703–712. [CrossRef]
24. Narayanaswami, S.; Rangaraj, N. Modelling Disruptions and Resolving Conflicts Optimally in a Railway Schedule. *Comput. Ind. Eng.* **2013**, *64*, 469–481. [CrossRef]
25. Zhan, S.; Kroon, L.G.; Veelenturf, L.P.; Wagenaar, J.C. Real-Time High-Speed Train Rescheduling in Case of a Complete Blockage. *Transp. Res. Part B Methodol.* **2015**, *78*, 182–201. [CrossRef]
26. Louwerse, I.; Huisman, D. Adjusting a Railway Timetable in Case of Partial or Complete Blockades. *Eur. J. Oper. Res.* **2014**, *235*, 583–593. [CrossRef]
27. Binder, S.; Maknoon, Y.; Bierlaire, M. The Multi-Objective Railway Timetable Rescheduling Problem. *Transp. Res. Part C Emerg. Technol.* **2017**, *78*, 78–94. [CrossRef]
28. Cadarso, L.; Marín, Á.; Maróti, G. Recovery of Disruptions in Rapid Transit Networks. *Transp. Res. Part E Logist. Transp. Rev.* **2013**, *53*, 15–33. [CrossRef]
29. Veelenturf, L.P.; Kidd, M.P.; Cacchiani, V.; Kroon, L.G.; Toth, P. A Railway Timetable Rescheduling Approach for Handling Large-Scale Disruptions. *Transp. Sci.* **2015**, *50*, 841–862. [CrossRef]
30. Zhu, Y.; Goverde, R.M.P. Railway Timetable Rescheduling with Flexible Stopping and Flexible Short-Turning During Disruptions. *Transp. Res. Part B Methodol.* **2019**, *123*, 149–181. [CrossRef]

31. Veelenturf, L.P.; Kroon, L.G.; Maróti, G. Passenger Oriented Railway Disruption Management by Adapting Timetables and Rolling Stock Schedules. *Transp. Res. Part C Emerg. Technol.* **2017**, *80*, 133–147. [CrossRef]
32. Haque, M.T.; Hamid, F.; Chaudhuri, A. A Rolling-Horizon Framework for Integrated Freight Train Rescheduling and Track Assignment under Disruptions in Large-Scale Networks. *Ann. Oper. Res.* 2026, *Early access*. [CrossRef]
33. Wang, R.; Zhou, M.; Wang, H.W.; Yang, B.; Dong, H.R.; Wang, F.Y. Coordinated Rescheduling of Train Timetable and Crew Scheme for Passenger-Freight Collinear Railway. *IEEE Trans. Comput. Soc. Syst.* **2024**, *11*, 5828–5838. [CrossRef]
34. Ghaemi, N.; Cats, O.; Goverde, R.M.P. Macroscopic Multiple-Station Short-Turning Model in Case of Complete Railway Blockages. *Transp. Res. Part C Emerg. Technol.* **2018**, *89*, 113–132. [CrossRef]
35. Altazin, E.; Dauzère-Pérès, S.; Ramond, F.; Tréfond, S. A Multi-Objective Optimization-Simulation Approach for Real Time Rescheduling in Dense Railway Systems. *Eur. J. Oper. Res.* **2020**, *286*, 662–672. [CrossRef]
36. Corman, F.; D'Ariano, A.; Marra, A.D.; Pacciarelli, D.; Sama, M. Integrating Train Scheduling and Delay Management in Real-Time Railway Traffic Control. *Transp. Res. Part E Logist. Transp. Rev.* **2016**, *105*, 213–239. [CrossRef]
37. Dollevoet, T.; Huisman, D. Fast Heuristics for Delay Management with Passenger Rerouting. *Public Transp.* **2014**, *6*, 67–84. [CrossRef]
38. Zhu, Y.; Goverde, R.M.P. Dynamic Railway Timetable Rescheduling for Multiple Connected Disruptions. *Transp. Res. Part C Emerg. Technol.* **2021**, *125*, 103080. [CrossRef]
39. Sato, K.; Tamura, K.; Tomii, N. A MIP-Based Timetable Rescheduling Formulation and Algorithm Minimizing Further Inconvenience to Passengers. *J. Rail. Transp. Plan. Manag.* **2013**, *3*, 38–53. [CrossRef]
40. Zhu, Y.; Goverde, R.M.P. Integrated Timetable Rescheduling and Passenger Reassignment During Railway Disruptions. *Transp. Res. Part B Methodol.* **2020**, *140*, 282–314. [CrossRef]
41. Altazin, E.; Dauzère-Pérès, S.; Ramond, F.; Tréfond, S. Rescheduling through Stop-Skipping in Dense Railway Systems. *Transp. Res. Part C Emerg. Technol.* **2017**, *79*, 73–84. [CrossRef]
42. Mavrotas, G. Effective Implementation of the ε-Constraint Method in Multi-Objective Mathematical Programming Problems. *Appl. Math. Comput.* **2009**, *213*, 455–465. [CrossRef]

Disclaimer/Publisher's Note: The statements, opinions and data contained in all publications are solely those of the individual author(s) and contributor(s) and not of MDPI and/or the editor(s). MDPI and/or the editor(s) disclaim responsibility for any injury to people or property resulting from any ideas, methods, instructions or products referred to in the content.